2017

IMPACT OF PRETREATMENT METHODS ON FAST PYROLYSIS OF BIOMASS

Yash Donepudi
Michigan Technological University, ydonepud@mtu.edu

IMPACT OF PRETREATMENT METHODS ON FAST PYROLYSIS OF BIOMASS

By

Yashwanth Donepudi

A DISSERTATION

Submitted in partial fulfillment of the requirements for the degree of

DOCTOR OF PHILOSOPHY

In Mechanical Engineering-Engineering Mechanics

MICHIGAN TECHNOLOGICAL UNIVERSITY

2017

This dissertation has been approved in partial fulfillment of the requirements for the Degree of DOCTOR OF PHILOSOPHY in Mechanical Engineering-Engineering Mechanics.

Department of Mechanical Engineering-Engineering Mechanics

Dissertation Co-Advisor: *Dr. Ezra Bar-Ziv*

Dissertation Co-Advisor: *Dr. Jordan Klinger*

Committee Member: *Dr. David Shonnard*

Committee Member: *Dr. Jeffrey Naber*

Department Chair: *Dr. William Predebon*

“This work is dedicated to my grandparents, Annapurna & Sri Hari Rao Alapati”

Table of Contents

List of figures

List of tables

Preface

This dissertation contains material from the manuscripts submitted to scientific journals as a result of collaborative work. Full citation details for these works are as follows:

Chapter 3:

DONEPUDI Y, ZINCHIK S, KLINGER J, BAR-ZIV E. 2017. BIOMASS PRETREATMENT METHODS FOR FAST PYROLYSIS. MANUSCRIPT SUBMITTED TO THE ELSEVIER JOURNAL, BIOMASS AND BIOENERGY.

Author contributions:

Donepudi- Experimental planning, collection of data, analysis and interpretation of data, writing of the paper

Zinchik- Experimental planning, collection of data, analysis and interpretation of data

Klinger- Experimental planning, analysis and interpretation of data, writing of the paper, paper review and editing

Bar-Ziv- Experimental planning, collection of data, analysis and interpretation of data, writing of the paper, paper review and editing

ZINCHIK S, KLINGER JL, WESTOVER TL, HERNANDEZ S, DONEPUDI Y, NABER JD, BAR-ZIV E. 2017. EVALUATION OF FAST PYROLYSIS FEEDSTOCK CONVERSION WITH A MIXING PADDLE REACTOR. MANUSCRIPT SUBMITTED TO THE ELSEVIER JOURNAL, FUEL PROCESSING TECHNOLOGY.

Author contributions:

Zinchik- Experimental planning, collection of data, analysis and interpretation of data, writing of the paper

Klinger- Experimental planning, collection of data, analysis and interpretation of data, writing of the paper

Westover- Analysis and interpretation of data, paper review and editing

Hernandez- Feedstock preparation

Donepudi- Feedstock preparation and collection of data

Naber- Analysis and interpretation of data, paper review and editing

Bar-Ziv- Experimental planning, analysis and interpretation of data, writing of the paper, paper review and editing

ZINCHIK S, ULLAL A, DONEPUDI Y, KLINGER JL, WESTOVER TL, BAR-ZIV E. 2017. HEAT TRANSFER ANALYSIS IN A PADDLE REACTOR FOR BIOMASS FAST PYROLYSIS. MANUSCRIPT SUBMITTED TO THE INTERNATIONAL JOURNAL OF HEAT AND MASS TRANSFER.

Author contributions:

Zinchik- Experimental planning, collection of data, analysis and interpretation of data

Ullal- Experimental planning, collection of data, analysis and interpretation of data, writing of the paper

Donepudi- Experimental planning, collection of data

Klinger- Analysis and interpretation of data, paper review and editing

Westover- Analysis and interpretation of data, paper review and editing

Bar-Ziv- Experimental planning, collection of data, analysis and interpretation of data, writing of the paper, paper review and editing

Chapter 4:

DONEPUDI Y, DESAI CK, ZINCHIK S, ULLAL A, KLINGER JL, BAR-ZIV E. 2017. ENHANCED BIO-OIL FROM ARUNDO DONAX. MANUSCRIPT SUBMITTED TO THE JOURNAL OF BIOFUELS, BIOPRODUCTS AND BIOREFINING.

Author contributions:

Donepudi- Experimental planning, collection of data, analysis and interpretation of data, writing of the paper

Desai- Experimental planning, collection of data, analysis and interpretation of data paper review and editing

Zinchik- Experimental planning, collection of data, analysis and interpretation of data

Ullal- Experimental planning, collection of data, analysis and interpretation of data

Klinger- Experimental planning, collection of data, analysis and interpretation of data, writing of the paper, paper review and editing

Bar-Ziv- Experimental planning, analysis and interpretation of data, writing of the paper, paper review and editing

Acknowledgements

I would like to acknowledge the financial support I received from my family, the Michigan Translational Research & Commercialization Program (MTRAC), Dept. of Mechanical Engineering-Engineering Mechanics of Michigan Technological University, National Science foundation (award# 1521383), Consortium for Advanced Wood-to-Energy Solutions (CAWES), Idaho National Laboratories and other public and private sponsors.

I would like to acknowledge the guidance and mentoring of my co-advisors Dr. Ezra Bar-Ziv and Dr. Jordan Klinger. I am grateful for your support and motivation provided to me throughout the course of my degree. Thank you for prioritizing my education and growth throughout the years. Also, I would like to acknowledge Dr. Naber and Dr. Shonnard for serving on my advisory committee, and for their careful review and support of my work.

I would like to acknowledge the many discussions and many contributions of my research colleagues; Chintan Desai, Ankith Ullal, Ulises Gracida Alvarez and particularly Stas Zinchik. I would like to thank our metal contractors, Dave Sladek and Nick Sladek from Universal Metal Works for their contributions in fabricating, repairing, replacing our lab equipment.

I would like to conclude by acknowledging the loving care and tireless support of my family and friends.

Abstract

Biomass is considered a renewable source of energy with minimum carbon foot print if managed sustainably. The majority of the worlds energy is spend on transportation, and fast pyrolysis of biomass could be a potential route for production of a sustainable liquid transportation fuel. However, there are several hurdles in the conversion process. This work addresses these hurdles by investigating the impact of several pretreatment methods on fast pyrolysis including thermal pretreatment (torrefaction), comminution/grinding, mineral reduction. The impact of important parameters like heat transfer medium, conversion temperature and particle size were also investigated.

A mild thermal pretreatment of biomass (~10-15% dry solids loss) had been proven to provide multiple benefits which include, reduction of grinding energy (~85% reduction), narrower particle distribution and production of bio-oils that have lower water and acid content, thus increasing stability. Comminution followed by mechanical sifting reduced the insoluble minerals (primarily silicon), which can cause damage to bio-refineries by increasing the equipment wear. More than 80% of the inorganics (both soluble and insoluble) were removed through aqueous high-shear mineral reduction technique when paired with mild thermal pretreatment. Removal of these soluble, structural minerals has decreased the amount of aqueous-fraction bio oils, and produced a higher quality oil.

Arundo Donax is a fast growing cane which is considered a low cost energy crop. However, its high mineral content made it less attractive for alternative bio-fuel

production. The high potential of the feedstock was the primary reason why this feedstock has been extensively studied in this work, and an effective pretreatment method to enable efficient conversion was sought. It was concluded that the particle size of the feedstock has minimal effect on the bio-oil yield within the studied range (<2 mm), whereas the conversion/reaction temperature had shown predominant effect. The optimal bio-oil yields for raw Arundo Donax were approximately 50-52% observed for feedstock with particle size in range of 0.425-0.850 mm at temperatures of 470-500 ºC. The high shear mineral reduction technique with multi stage fast pyrolysis was also investigated with up to approximately 40% dry solids loss in first stage (torrefaction). It was found that the mineral reduction increased the liquid product yield (up to 62%), approaching that of clean woody feedstocks. This work indicated that the liquid yield can be effectively fractionated through sequential degradation stages without losing the product yield.

In conclusion, the presented work in this dissertation indicates that integration of pretreatment methods like mineral reduction, comminution and thermal treatments with fast pyrolysis enables the use of low cost biomass feedstocks to be able to produce stable bio-oils with optimal yields. Further, this work demonstrates, in part, that the presented (relatively) simple and low-cost conversion reactor can produce a high yield of liquid pyrolysis oil from a range of woody, herbaceous, and agricultural residues and wastes. Sequential staging of these reactors can produce a thermally fractionated product.

1 Introduction

Mankind is always in search of new sources. With ever increasing population, there is an exponential increase in the need for energy, and exploring different energy resources. Today, more than 70% of the energy in the world is extracted from fossil fuels like coal, petroleum and natural gas (EIA 2016). Although fossil fuels have attractive calorific values, their carbon cycle is contained in a carbon cycle that is not considered renewable due to the very long time-horizon.

1.1 Motivation

Figure 1.1 shows the world's energy consumption by energy source, which have projections till the year 2040 (EIA 2016). It can be observed that the largest energy suppliers are liquid fuels (predominantly for transportation and industry) which is increasing with a rate of 1%/year. However, the coal consumption is projected to decrease by 21% by 2020 and 24% by 2040 compared to the reference values taken in 2012. This decrease in usage of coal for energy is compensated by increasing natural gas consumption and increase of renewable energy. It was projected that the energy from renewables will increase by 7% by 2020 and to a staggering 37% by 2040 compared to 2012. The plot also shows the minimal impact of Clean Power Plan (CPP) on the energy consumption from coal and renewables compared to the original projections, where it shows that the plan neither reduces the coal consumption nor increase the consumption of renewables. Figure 1.2 shows the total energy produced by different renewable sources from year 2000 until 2016 (EIA 2017), where it can be seen that energy from biomass

occupies the top place. The energy from biomass in 2016 had registered an increase by a factor of 1.6 compared to 2000, and is projected to grow.

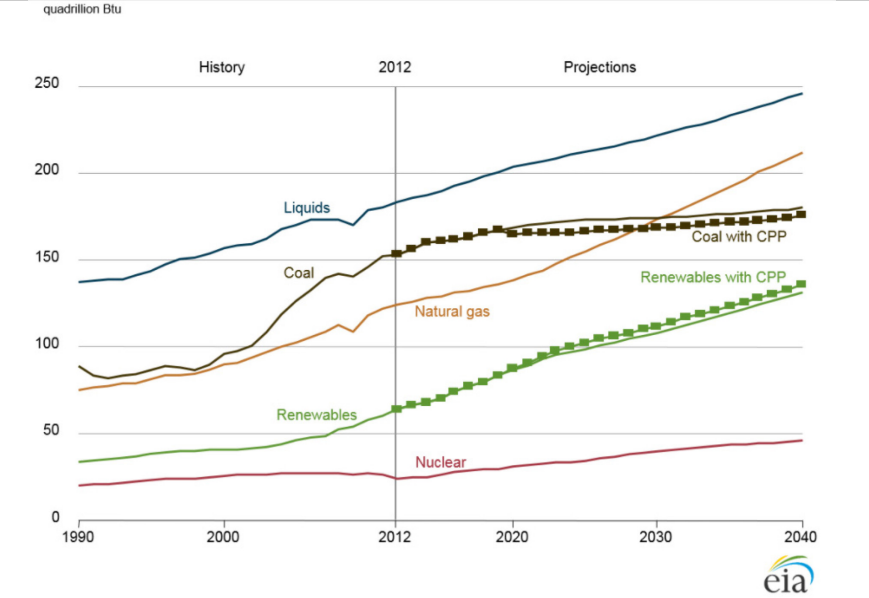

Figure 1.1 World energy consumption by energy source (EIA 2016) (Reprinted with permission from EIA)

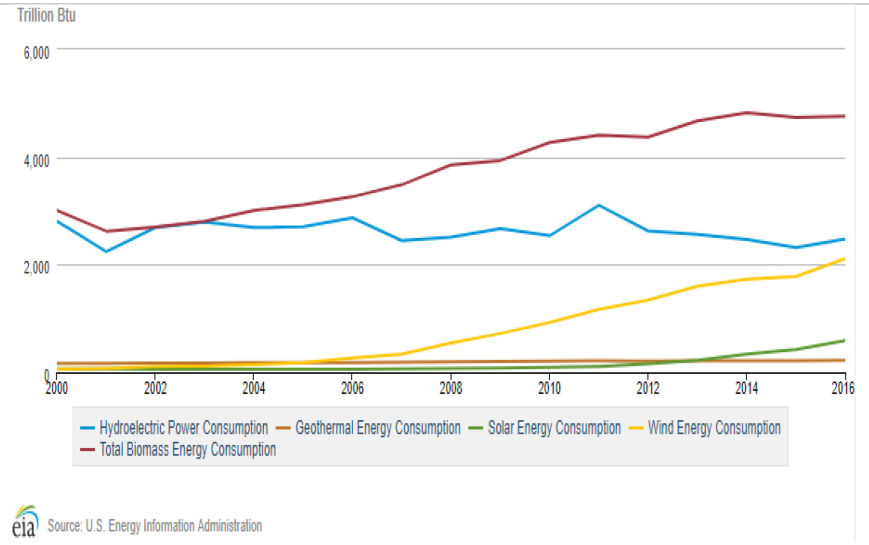

Figure 1.2 Total energy production from different renewables from year 2000 to 2016 (EIA 2017) (Reprinted with permission from EIA)

The emphasis of this work is on using biomass as a feedstock to produce alternate fuels. Biomass is capable of providing renewable energy as it can be replenished within a sustainable, short time-horizon carbon cycle unlike fossil fuels. Biomass derived fuels have a benefit of reduced greenhouse gas emissions compared to fossil fuels and are considered as carbon neutral (Skone 2012). From the data published by the U.S. Energy Information Administration, the world's total energy consumption from renewable fuels in the year 2015 was 12.5% and is projected to slightly increase to approximately 18% by 2050 (EIA 2016). From this data it can be understood that renewable energy is not going to satiate the entire energy requirement of the world, however it can be used to increase energy self-sufficiency of the nation by providing an alternative source of energy and reducing overall energy imports. Figure 1.3 shows the slow growth of U.S. rural employment rate compared to urban areas, which were almost the same before the recession in 2008 (USDA 2017). After that the rural employment rate suffered a huge hit and is struggling to improve. Creation of new biomass energy based industries in and around rural places can enhance the growth of small towns in terms of job creation and overall development of these areas.

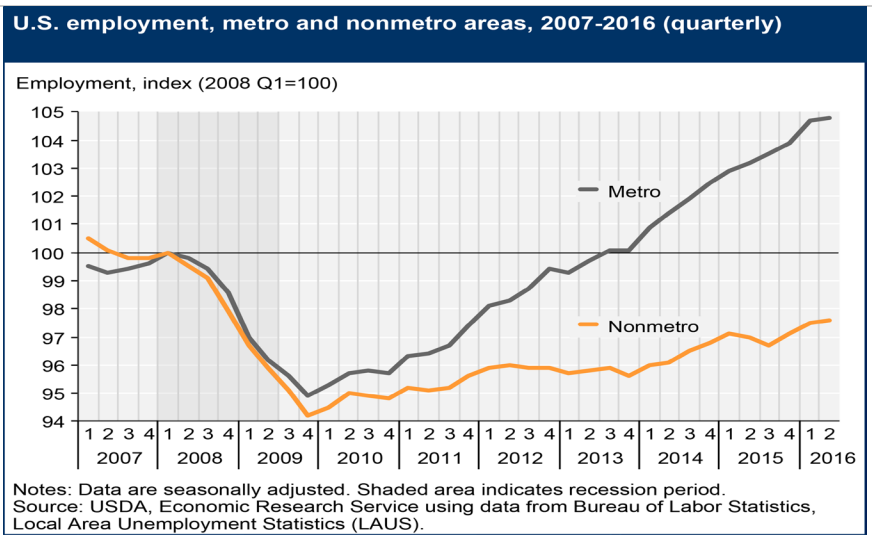

Figure 1.3 U.S. employment rates from year 2007 to 2016 (USDA 2017) (Reprinted with permission from USDA)

1.2 Thermochemical conversion

Biomass can be converted in fuels by various methods such as decomposition, fermentation, thermochemical conversion etc. Thermochemical conversion of biomass is an age old process where it was traditionally used to produce a high quality solid fuel through heating the biomass in an oxygen deficient environment. More advanced techniques and process that increase the productivity and quality are recently being developed and is becoming a near-term solution to produce biological based replacements for fossil fuels. This work deals with two important thermochemical processes namely torrefaction and fast pyrolysis.

1.2.1 Torrefaction

Torrefaction is a mild pyrolysis process that occurs in the temperature range 200-300 ºC in inert environment to primarily produce a solid product (Acharya, Sule et al. 2012).

Torrefied biomass has improved properties in handling, conveying, downsizing, blending and enhanced properties in downstream products (Acharya, Sule et al. 2012). The most common feedstock for this process is lignocellulosic biomass, which consists of three main polymeric components: cellulose, hemi-cellulose and lignin. In the ideal torrefaction process, a large portion of the hemi-cellulose and a very small portion of cellulosic and lignin are thermally degraded to create a fuel with optimum desirable characteristics. The torrefaction process is influenced by important parameters like temperature, residence time, local gaseous environments (sweep gases) and pressure. These parameters have been shown to affect the chemical composition of the final product from this process (Bergman, Boersma et al. 2005). Torrefaction improves many characteristics of biomass like heating value, hydrophobicity (Bergman, Boersma et al. 2005), grindability (Bridgeman, Jones et al. 2010, Phanphanich and Mani 2011) and particle size distribution upon size reduction (Phanphanich and Mani 2011).

1.2.2 Fast pyrolysis

Fast pyrolysis is thermochemical conversion process taking place at high temperatures in range of 400-700 ºC with a short residence time of 0.5-10 s in absence of oxygen. Fast pyrolysis usually involves small particles (<1 mm) to assist in achieving high heating rates of >10 K/s, which is crucial to preferentially yield a large quantity of product liquid. Fast pyrolysis is considered as one of the promising pathways to create transportation fuels (Mohan, Pittman et al. 2006). The three products from biomass fast pyrolysis are char, bio-oil and gases. The prime product is the liquid oil which can be further catalytically refined to create liquid fuels, whereas the solid char can be used as activated

carbon in filtering devices, as a soil amendment, as a reductant in metal foundries, or as a solid fuel. The non-condensable gases are typically combusted as a low-value gas stream to provide process heat.

1.3 Objectives

The primary goal of this work is to enhance the state of knowledge and advance the development and deployment of fast pyrolysis. This work seeks to enable the use of low-cost biomass feedstock for the production of high-quality bio-oils. This is accomplished through the development, analysis, and demonstration of various biomass fast pyrolysis pretreatment methods and the subsequent thermochemical conversion. The main objectives of this work are;

1. To develop and explore pretreatment methods for fast pyrolysis to enable the use of low cost feedstock and enhance fuel quality.
2. To develop and operate a fast pyrolysis reactor to achieve efficient thermochemical conversion.
3. To study a new feedstock that is an energy crop rich in minerals for production of enhanced pyrolysis oil.

1.4 Dissertation structure

This dissertation consists of five chapters. The structure of the report is shown in Figure 1.4. The work reported in chapter 3.2 (shown in red in the figure) was a collaborative effort led by Stas Zinchik of Michigan Technological University and the author of this dissertation participated in this effort.

Chapter 1 includes the motivation for this work and research objectives. Chapter 2 consists the details of the comprehensive literature survey conducted with regards to the research objectives with a goal to find the knowledge and technological gaps in the field of study.

Chapter 3 comprises all the details with regards to experimental research done during this work, which is divided into three parts. Chapter 3.1 includes the investigation and analysis of the three pretreatment methods i.e. comminution, torrefaction and mineral removal. Chapter 3.2 provides the details of the design, operation and thermal analysis of the new mixing paddle reactor used for this work. Chapter 3.3 provides details into fast pyrolysis processing of biomass.

Chapter 4 comprises of all the work done with Arundo Donax (AD) as the feedstock (with reference to objective 3). The work presented in this chapter includes the parametric study and investigation into the effect of minerals and torrefaction on AD fast pyrolysis.

Chapter 5 provides the conclusions from this work and suggestions for future work.

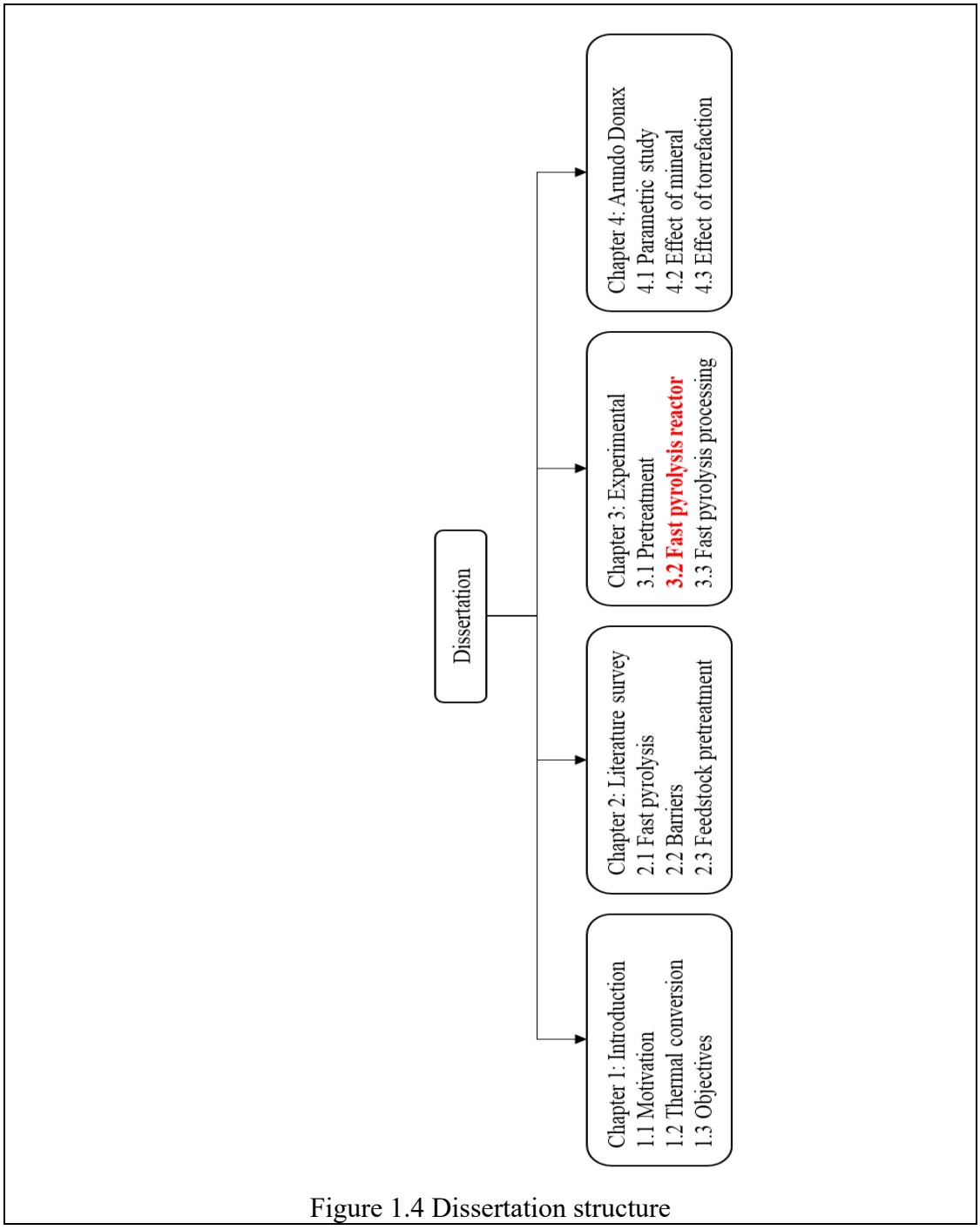

Figure 1.4 Dissertation structure

2 Literature survey

2.1 Fast pyrolysis

2.1.1 Definition

A thermal decomposition in absence of oxygen with moderate reaction temperature and short residence time to primarily produce liquid product is known as fast pyrolysis (Bridgwater 2012). As with any pyrolysis process, fast pyrolysis also produces solid and gaseous fractions. The liquid product is known as pyrolysis oil or bio-oil, whereas the solid and gaseous fractions are known as char and non-condensable gases respectively. The typical yields from biomass fast pyrolysis are given in Table 2.1.

Table 2.1 Typical yields from biomass fast pyrolysis (Brown and Holmgren 2009)

Product	**Yield**
Oil	60-70%
Char	12-15%
Gas	13-25%

2.1.2 Review

The major advantages of biomass fast pyrolysis are that the operation can take place at atmospheric pressure at a moderate reaction temperatures (450-600 ºC) and can produce very good liquid yields exceeding 70 wt% depending on the feedstock type. The drawbacks include high oxygen and water content with a phase separation, polymerization and corrosion. (Brown and Holmgren 2009)

All the three products from fast pyrolysis of biomass have applications. Bio-oil can be used as a fuel by itself in boilers, as co-fuel in co-firing, turbines. It can be further upgraded to produce transportation grade fuels to be used by internal combustion engines. Bio-char has similar fuel properties as lignite and can be used as a low grade

process fuel in the fast pyrolysis bio-refinery to recuperate some energy. Activated carbon can be made easily from bio-char which has many applications in water filtration, fertilizer industries. The non-condensable gases can be recycled to be used as a source of energy in the process in large scale settings. Recycling non-condensable gases into the reaction chamber during catalytic fast pyrolysis of hybrid poplar was studied by Mante et al. which has resulted in increased heating value and pH of the bio-oil, and reduced its viscosity, density and oxygen content (Mante, Agblevor et al. 2012). (Dhyani and Bhaskar 2017)

Most of the properties of bio-oil like oxygen content, water content, volatility, viscosity and corrosiveness depending on the feedstock and process parameters like reaction temperature, residence time and heating rates.

Bio-oils consists 35-40 wt% of oxygen, which is one of the reasons (including with high water content) for its inferior properties compared to hydrocarbon/petroleum derived liquid products. The high oxygen content leads to loss of heating value and is the prime cause for instability of the bio-oil while it's aging. High reaction temperatures can reduce the amount of oxygen content while sacrificing the total oil yield from the cracking of pyrolysis vapors. (Czernik and Bridgwater 2004)

The water content in the bio-oil is a result of dehydration and the moisture present in the feedstock during pyrolysis which account to 15-30 wt% of the original sample. The water in bio-oil forms a homogenous mixture with lignin based oligomeric compounds due to the effect of low molecular weight acids, alcohols, hydro-aldehydes and ketones

produced as a result of carbohydrate decomposition. (Czernik and Bridgwater 2004) The water in the bio-oil has a negative effect of several fuel properties such as heating value, flame temperatures, ignition delays and combustion rates compared to similar petroleum fuels like diesel fuel (Elliott 1994). However, it does have a positive effect on helping the flow characteristics of bio-oil by reducing its viscosity and helps improve the atomization property of the oil which helps in uniform temperature distribution across the combustion chamber encouraging lower NO_x emissions. (Czernik and Bridgwater 2004)

Due to high amounts of non-volatile compounds like sugars and phenols, bio-oil presents a poor volatility which can foster the formation of soot/residue after combustion. On other hand, the viscosity of bio-oil varies depending on feedstock and other process parameters. Compared to traditional hydrocarbon oils, the viscosity of bio-oils reduces with increase in temperature for transportation/pumping purposes. However, the viscosity of bio-oils increase with aging when stored at high temperatures due to the formation of macro-molecules as a result of chemical reactions and oxygen exposure. (Czernik, Johnson et al. 1994, Czernik and Bridgwater 2004)

Bio-oil consists of carboxylic acids like acetic and formic acids which make the oil acidic with a lower pH (2-3) which makes it extremely corrosive and needs special containers for storage, transport and handling. (Dhyani and Bhaskar 2017)

2.2 Barriers

2.2.1 Feedstock variety and costs

Several factors influence the quality and quantity of biomass feedstocks like growing conditions, harvesting techniques, weather, storage conditions, and demand from existing biomass based industries like lumber and paper, leftover wastes from sources like agriculture, municipalities etc. and pretreatment methods used before fuel processing. These factors will determine price of the feedstock where high quality feedstocks (low ash and moisture content) like woody feedstocks (used in lumber and paper mills) tend to be more expensive compared to low cost feedstocks like herbaceous type (agricultural wastes, MSW etc.). However, obtaining a singular feedstock for fuel production is not possible on a large scale due to regional variability and availability, growing rates and logistics costs. This is the prime reason for using biomass blends in fast pyrolysis. (Thompson, Aston et al. 2017)

Kenney et al. have extensively studied biomass feedstock variability and provided three major factors which differentiate biomasses i.e. ash content, sugar content, particle morphology and moisture content (Kenney, Smith et al. 2013).

Ash content in biomass varies depending on its sources. Two main routes for ash content are from external and internal factors. External sources such as blowing wind, certain harvesting methods increase the chance of soil contamination which increases the total silicon content of the feedstock. Mineral up take by the feedstock for its nourishment from the soil is considered as the ash from internal factors which is known as structural ash. Ash in excess amount can cause excessive wear of the material handling systems,

reduced thermal conversion efficiencies by reducing the oil yields and increasing the acid content, slagging and fouling of the boilers and disposal costs arising from using fuels produced such feedstocks. The ash content of the feedstock can be reduced by using techniques like proper fractionation and agronomic management practices which will reduce the external factors like soil contamination, and preprocessing techniques like acid/water leaching to remove internal/structurally bound minerals. (Kenney, Smith et al. 2013)

Sugars in biomass vary significantly with the type of biomass. Biochemically produced liquid fuels yields predominantly depend on the amount of sugars present in the feedstock. Lower sugar content leads to lower yields. The major factor effecting the sugar content of the feedstock, beyond the plant genomics, is storage. Proper storage techniques will preserve the carbohydrates present in the feedstock. Feedstock blending can also compensate the loss of sugars, thereby encouraging feedstock with uniform sugar content. (Kenney, Smith et al. 2013)

Size, shape and density (particle morphology) also play a major role in conversion processes. It is also a key factor in material handling where it can affect the throughput of the conversion facility. The material properties and operating parameters of size reduction systems are interlinked, which makes it very difficult to control the particle morphology of feedstocks. This inefficiency can directly show impact on plant economics. The solution for this is to use consistent preprocessing techniques with properly engineered material handling/feeding systems. (Kenney, Smith et al. 2013)

Moisture content is one of the important parameters that vary in feedstocks. It is also one of the difficult varying parameters to control as it is directly affected by the environment. Feedstock moisture can cause corrosion and blockages inside the preprocessing equipment like grinders/mills and material handling systems. It increases the water content of the bio-oil which reduces its heating value. Good harvesting and storage practices with state of the art preprocessing and handling systems are a few solutions to mitigate the problems with varying moisture content in the feedstock. (Kenney, Smith et al. 2013)

2.2.2 Technology considerations

2.2.2.1 Cost barriers

In 2013, Jones et al. studied the process design and economics related to the conversion of biomass into hydrocarbon fuels. They assumed a bio refinery that uses that has a capacity of processing 2,000 tons of dry tons biomass per day, which resulted in a yield of 40 and 44 gallons of gasoline and diesel blend stock respectively. The study found out that the minimum selling price of the fuel was $3.39 per gasoline gallon equivalent (2011 U.S. dollar value), which is higher than the price of traditional gasoline. The single most significant cost was from feedstock and its handling which was given as $0.92 per gasoline gallon equivalent. (Jones, Meyer et al. 2013)

In 2015, Dutta et al. used the above study to research pathways with in situ and ex situ upgrading of fast pyrolysis vapors with similar goal to provide economics for the conversion of biomass into hydrocarbon fuel. The study found that by 2022, the

minimum selling price of the fuel was $3.46 per gasoline gallon equivalent when in situ catalyst path was chosen whereas the price was $3.31 per gasoline gallon equivalent for ex situ catalyst case. The study also found that ex situ is preferred over in situ for fuel production from biomass as it encouraged the production of higher distillate products while favoring the reactions for hydrogenation and hydrodeoxygenation. Also the operating costs of catalysts in ex situ case are lower compared to in situ as it has lower probability of catalyst poisoning and maintenance. The feedstock and its handling costs still occupy the prime share of the fuel cost with an average cost of $1.04 per gasoline gallon equivalent, which is 30% of the total fuel cost. (Dutta, Sahir et al. 2015)

From these studies it is inferred that in the future, the price of biomass derived fuel obtained by fast pyrolysis will be competing with the traditional gasoline price, however the cost of feedstock remains a major hindrance.

2.2.2.2 Technologies

There are several reactor technologies available for fast pyrolysis. The most common reactors are bubbling fluidized bed, circulating fluidized bed, rotating cone pyrolyzer, ablative pyrolyzer, vacuum pyrolysis and auger reactor. (Brown and Holmgren 2009)

2.2.2.2.1 Bubbling fluidized bed

This is one of the most popular reactor technologies in the field of fast pyrolysis. The heat is externally supplied to the bed of the reactor. The high velocity of the hot fluidizing gas will ensure good mass and heat transfer during the process, however it

requires very high carrier gas supply and uniform biomass particle size. These type of reactors are easily scalable. (Brown and Holmgren 2009)

2.2.2.2.2 Circulating fluidized bed

This reactor technology is similar to that of the bubbling type the only difference being that it has a heat transfer medium such as sand that is circulated between the reaction and combustion chamber. The heat for the process is supplied by combusting the char from the process. The main advantage of this technology is that it provides high throughputs and easily scalable. As with the bubbling type, these reactors do need high amounts of carrier gas and cause char attrition. (Brown and Holmgren 2009)

2.2.2.2.3 Rotating cone pyrolyzer

This type of reactor uses small biomass particles. The biomass particles come into contact with a heat transfer medium (like sand) in a rotating cone reactor. This type of reactor does not require carrier gas and has a compact design, however it suffers from difficulty in scaling. (Brown and Holmgren 2009)

2.2.2.2.4 Ablative pyrolyzer

In this type of reactor, the biomass particle is pressed onto a hot rotating disc with certain pressure, which creates the required reaction temperature for producing liquids. The advantages of this type of reactor are that it can use large particles and does not require carrier gas. The technology is complex and hard to scale up. (Brown and Holmgren 2009)

2.2.2.2.5 Vacuum pyrolysis

This reactor technology uses a multiple hearth reactor with rotating scrappers. The biomass particles are moved by gravity through different hearths maintained at different temperatures increasing from 200 ºC to 400 ºC. The vapors and aerosols are pumped into condensers using a vacuum pump. These type of reactors need carrier gas (lower amounts) and can accept larger biomass particles. These are expensive and is difficult to scale up. (Brown and Holmgren 2009)

2.2.2.2.6 Auger reactor

This type of reactor uses a screw conveyor (auger) to mix and carry the biomass and heat transfer medium. They require minimal amount of carrier gas and need to preheat the heat transfer medium prior to making contact with biomass particle. These reactors are easy to scale up and uses small biomass particles. The bio-oil yield is reduced compared to bubbling and circulated fluidized bed reactors. (Brown and Holmgren 2009)

Table 2.2 Commercial attractiveness of fast pyrolysis reactor technologies (Brown and Holmgren 2009)

Reactor	**Fluid bed**	**Circulati-ng fluid bed**	**Rotatin-g cone**	**Ablative**	**Entra-ined flow**	**Cyclon-ic**	**Auger**
Technology strength	Strong	Strong	Average	Average	Weak	Strong	Strong
Market Attractiveness	High	High	Average	Above average	Low	Above average	High

Table 2.2 shows the technology strength and commercial attractiveness of all the available popular fast pyrolysis reactor technologies. It can be observed that fluid bed, circulating fluid bed and auger reactor technologies have higher chances commercial acceptance.

2.2.2.3 Auger reactor review

Ingram et al. studied the possibility of a portable fast pyrolysis technology using auger based reactor to be used in forests to obtain bio-oil at the source (on site) to reduce the costs of transporting less dense raw biomass to a processing facility. They studied four different woody feedstocks (pine wood, pine bark, oak wood and oak bark) where they pyrolyzed them at reaction temperature of 450 ºC. The results from auger pyrolysis were comparable to fluidized bed and vacuum pyrolysis, however the heating rates were lower than those from the fluidized bed reactors. (Ingram, Mohan et al. 2007)

Puy et al. studied the valorization of pine wood chips using an auger reactor at different temperatures from 500 ºC to 800 ºC with varied residence time (5-1.5 minutes). They observed that the maximum oil yield from pine wood chips using an auger reactor was 59% (wt%), which was achieved using the reaction temperature of 500 ºC and a residence time of >2mins. (Puy, Murillo et al. 2011)

Sirijanusorn et al. studied the pyrolysis of cassava rhizome in a counter rotating twin screw reactor using various reaction temperatures, particle sizes and carrier gas pressures. They found that maximum oil yield for cassava was obtained using reaction temperature of 550 ºC with a particle size of 0.250-0.425mm. The important findings from this study is that the water content of the bio-oil reduced when compared to the results produced by fluidized bed and single screw reactors compared from literature. However, there is a significant increase in solid fraction (char). (Sirijanusorn, Sriprateep et al. 2013)

The common notion observed from auger reactor literature is that these type of reactors are capable of producing comparable oil yields with fluidized bed reactors, however they may require a heat transfer medium and better mixing characteristics to improve the heating rates and oil yields.

2.2.3 Stability and corrosion

Bio-oils are inherently unstable with regards to thermodynamic equilibrium. Many reactions will take place during storage of the bio-oil as the oil ages/matures. The instability of bio-oil can be seen as a slow increase of viscosity with storage time, rapid increase of viscosity by heating and evaporation of volatiles and oxidation with air. (Oasmaa and Kuoppala 2003)

Diebold reviewed chemical and physical mechanisms of the storage stability of fast pyrolysis oils. It was found that chemical reactions may take place while the bio-oil is aging. It was found that the most unstable compounds were aldehydes, where they can react with water/phenols/alcohols/proteins to form hydrates/resin+water/hemiacetals, acetals+water/oligomers, resins respectively. The acid can react with alcohols to form water and esters whereas mercaptans can react to form dimers and olefins can react to form polymers. The exposure to air can provide oxygen to oxidize the oil to form more reactive acids and peroxides that may act as catalysts for polymerization of certain compounds. The entrained char particles may contain catalyst minerals (such as K, Na) which will encourage these adverse reactions. (Diebold 1999)

Similar observations were made by Oasmaa and Kuoppala, where they observed that majority of the physiochemical changes occur in first 6 months of storage. They observed the increase in high molecular mass lignin compounds with reducing aldehydes, ketones and monomers. They recorded an increase in density, viscosity and flash point, where the heating value was decreased. (Oasmaa and Kuoppala 2003)

Meier et al. studied several compounds of bio-oil for 32 weeks stored at different conditions and concluded that cooling will help delay the polymerization reactions, however it could not eliminate the reactions. (Meier, Jesussek et al. 2003)

Fratini et al. concluded that ageing of bio-oil may be defined as the process of agglomeration of macro lignin molecules and will continue until it separates from the lighter oil fraction. (Fratini, Bonini et al. 2006)

Elevated temperatures will rapidly increase the ageing process of bio-oil. Oasmaa et al. observed the four quintessential ageing signs i.e. thickening of macro lignin molecules, phase separation, viscous formation of pyrolytic lignin and char formation from the respective viscous lignin at high temperatures. (Oasmaa, Leppawaki et al. 1997)

Boucher et al. studied bio-oils stored at two different temperatures i.e. 50 ºC and 80 ºC for a week and observed that bio-oil showed rapid ageing/change in properties at 80 ºC and no significant changes at 50 ºC. (Boucher, Chaala et al. 2000)

Thermal stability of bio-oils with higher extractives was studied by Chaala et al., where they had observed that the change in molecular weight of the bio-oil stored at 80 ºC for a

week is similar to that of the one stored at room temperature for a year. (Chaala, Ba et al. 2004)

Bio-oils have a pH of 2-3 and an acid number of 50-100 mg KOH/g, which translated into very acidic and corrosive (Oasmaa and Czernik 1999). Also the severity of the corrosion increases with temperature and water content in the bio-oil (Aubin and Roy 1990). Stainless steel is not affected by the corrosiveness of bio-oils (Oasmaa and Czernik 1999). Brady et al. studied the impact of bio-oil corrosiveness on different stainless steel alloys (409, 410, 304L, 316L, 317L and 201) and concluded that the least effected alloys was 201 (thinnest oxide layer), it was due to the availability of Cr to be able to form an protective layer as the Mn in the alloy absorbs the S particles, thereby limiting the formation of Cr-S which reduced the corrosion resistance in other alloys (Brady, Keiser et al. 2017).

2.2.4 Upgrading requirements

The properties like high oxygen, water and acid content make the bio-oil undesirable to be used as a substitute for traditional petroleum fuels. For this reason the raw bio-oil needs to be upgraded to have reduced oxygen and water content.

The most popular bio-oil upgrading techniques are hydrodeoxygenation, catalytic cracking of pyrolysis vapors and emulsification.

Hydrodeoxygenation: The hydro-process where the hydrogen is forced into the bio-oil to remove/reduce the oxygen content into H_2O and CO_2 with the help of catalysts under pressure, thereby increasing the heating values is known as hydrodeoxygenation (Zhang,

Chang et al. 2007). By using sulphided Co-Mo-P/Al_2O_3 catalyst, Zhang et al. were able reduce the oxygen content of the bio-oil (dewatered) from 41.8% to 3% by hydro-treatment (Zhang, Yan et al. 2005). Excessive cost, complex technology, catalyst deactivation and reactor clogging are the main hindrances of using hydro-treatment of bio-oils.

Catalytic cracking of pyrolysis vapors: This is the process where there is a catalytic decomposition of oxygen rich bio-oil vapors into hydrocarbons and H_2O, CO_2/CO. Nokkosmaki et al. studied the effect of ZnO catalyst on composition and stability of bio-oils and observed that the catalyst had decomposed anhydrosugars and did not affect the lignin compounds and the process deactivated the catalysts. However, when tested for viscosity change after heating the ZnO treated and untreated oils at 80 ºC for 24 hours; the treated sample had lower increase in viscosity compared to untreated sample showing the increment in the stability of treated oil (Nokkosmäki, Kuoppala et al. 2000). Adjaye and Bakhshi studied five different catalysts for catalytic upgrading and concluded that HZSM-5 was the best catalyst to produce oil with high hydrocarbons with least char formation (Adjaye and Bakhshi 1995, Adjaye and Bakhshi 1995). Catalytic upgrading is comparatively cheaper to other bio-oil upgrading techniques, but suffers with high char formation and frequent deactivation of catalysts.

Emulsification: Combining bio-oils with traditional petroleum fuels (like diesel) is known as emulsification. Chiaramonti et al. studied the effect of different bio-oil wt% emulsion ratios with diesel and found that the emulsions are much more stable than the raw bio-oil and found the optimal viscosity range between 0.5-2% to be used in diesel engines

(Chiaramonti, Bonini et al. 2003, Chiaramonti, Bonini et al. 2003). Emulsification is a simple process but takes a lot of energy to prepare a proper emulsion. Corrosion is reduced in emulsion based fuels, however the concentrations of strong acids still present within may not be neglected as it effects the engine components (Zhang, Chang et al. 2007).

2.3 Feedstock pretreatment

2.3.1 Definition

Feedstock pretreatment is a set of processes that the feedstock undergoes before being converted into a fuel. It is a very broad term and can be used to define one or many processes working to produce a better fuel in terms of quality and quantity.

There are several different biomass pretreatment processes, of which the most important being grinding, drying, torrefaction and mineral removal. Depending on the process of producing final product any or all of these processes can be referred as feedstock pretreatment. In this work the emphasis is on studying the impact of above mentioned pretreatment processes (primarily grinding, torrefaction and mineral removal) on fuels produced by fast pyrolysis.

2.3.2 Grinding and downsizing

Grinding of biomass is one of the most important pretreatments as the size of the biomass particle is crucial in having an efficient process of optimal fuel extraction. Smaller sizes enhance the possibility of having the entire biomass fiber to participate in the reaction (higher heating rate) whereas larger particles might inhibit this in given time. The

residence time might have to be increased depending on the reactor technology to completely process larger particles, which may have an effect on the throughput of the facility. However, size reduction comes with a significant price tag in terms of energy consumed by the size reduction equipment (grinders, mills etc.) as biomass is fibrous in nature.

To save on energy, the literature suggests to use torrefaction before grinding as the thermal process weakens the fibers thus reducing the grinding costs significantly. (Phanphanich and Mani 2011) Depending on the torrefaction severity, one can achieve 10 times reduction in specific grinding energy using torrefied compared to raw biomass (Phanphanich and Mani 2011). There should be a fine balance made in terms of choosing the torrefaction severity to benefit the grinding energy usage as the severity increases the total energy yield from the feedstock decreases due to the loss of volatiles during the thermal degradation. A severe torrefaction temperature of 300 ºC will result in on an average energy yield of 70% (~50% mass loss) compared to 90% (~20% mass loss) with mild torrefaction temperatures of 250 ºC (Arias, Pevida et al. 2008, Bridgeman, Jones et al. 2010, Phanphanich and Mani 2011, Colin, Dirion et al. 2017). It was studied that on a large scale basis, the auto thermal process where the volatiles lost from torrefaction process were recycled and used as a heating source can outweigh the drawbacks of energy loss/consumed during torrefaction and other precursor processes like drying and grinding and can result in a total net process efficiency of 92% (Bergman, Boersma et al. 2005).

Salehi et al. studied the effect of different operating parameters on the yield and quality of bio-oil produced from saw dust and concluded that reaction temperature and feedstock particle size play a crucial role in providing good yields of quality bio-oil. Processing smaller particle sizes (< 590 microns) have produced more bio-oil compared to larger particles (590-1400 microns) as a result of high heating rates and reduced the bio-char and non-condensable gas yields (Salehi, Abedi et al. 2011). The particle size also have an influence on the total water content in the bio-oil, where smaller particle sizes yielded lower water content compared to large particle size (Salehi, Abedi et al. 2011). Smaller sizes also have positive effect (increasing) on pH, carbon content and heating value compared to large particles (Salehi, Abedi et al. 2011).

Jiang et al. studied the effect of combined torrefaction and ex-situ grinding pretreatment on Mallee wood and concluded that using feedstock pretreated with torrefaction temperatures of 260 ºC and subsequent grinding have produced higher bio-oil and lower char yields, however this beneficial effect was diminished when the torrefaction temperature was increases, where the higher temperatures increased the charring reactions leading to higher char and lower bio-oil yields (Jiang, Hu et al. 2017).

From the literature, it can be inferred that the combination of torrefaction and grinding will enhance the quality and quantity of bio-oil. The proper parameters for this mild thermal pretreatment and grinding depend on type of feedstock.

2.3.3 Mineral removal

By its very nature biomass has minerals, especially alkali and alkaline earth metals (AAEM's). Several of these minerals are used by the biomass for its growth and nourishment. The minerals can be found in the soil the biomass grows on or from external sources like fertilizers in case of agricultural based biomass. Combustion of fuels derived from these mineral rich feedstocks may cause a serve corrosion of the combustion chamber (example: boilers) in form of slagging and fouling. This corrosion will be responsible for derating of the power system by lowering the overall efficiency and can cause severe damage to the interior walls of the chamber. Often low cost feedstocks are high in mineral content like agricultural wastes, municipal solid wastes, which will serve as a major disadvantage to use the cost effective feedstocks.

Baxter et al. studied the behavior of inorganic minerals in biomass fired power boilers and concluded that potassium in the biomass is the mineral causing maximum damage to the power system by causing corrosion in terms of fouling (Baxter, Miles et al. 1998). They studied several biomasses and gave the inherent potassium content as 1% (of dry fuel wt.) for herbaceous and 0.1% for mature woody fuels. They also observed that the fuels rich in potassium also have higher concentrations of chlorine, sulfur and silicon, which are commonly known to react with potassium to form corrosive compounds (Baxter, Miles et al. 1998).

Leaching of biomass is a widely used mineral reducing pretreatment method, where the biomass is soaked in solvents or acidic solutions for a specific time and temperature. Solvent leaching (usually with water) is capable of reducing water soluble minerals like

potassium and acidic solutions are typically used to remove insoluble minerals like silicon, calcium etc.

Tonn et al. studied the effect of water leaching on fresh and dried biomass and concluded that water leaching may be only effective on dried biomass (Tonn, Dengler et al. 2011). Jenkins et al. also studied water leaching of biomass and were able to achieve a potassium removal efficiency of 90% just by soaking biomass (straw from Japonica) in deionized water at room temperature, however the process took a very long time (24hrs) and heavy water to biomass ratio (35:1) (Jenkins, Mannapperuma et al. 2003).

Saddawi et al. studied several varieties of biomass and their mineral content with its effect on respective derived fuel. One of their finding was that herbaceous biomasses typically have more water soluble minerals than woody biomasses. They also studied water and acid leaching and had good mineral removal efficiencies (62% of K to 100% of Cl) with reasonable water to biomass ratio of approximately 17:1, however the residence times are very long ranging from 20 hr. to 60 hr. depending on the type of leaching. They found that high mineral content reduces the ash fusion temperature of the fuel, thereby enhancing its corrosion ability. Reduced mineral content biomass showed lower reaction rates to thermal degradation as a result of lower catalytic ions from minerals like potassium. (Saddawi, Jones et al. 2012)

Several studies were done to study the effect of AAEM's on thermal decomposition characteristics of biomass. Eom et al. found that the reduction in mineral content of biomass through different mineral removal techniques (water and acids) had assisted in

lowering the low molecular compounds like organic acids and increasing useful sugars like levoglucosan during pyrolysis, however the reduced minerals causes a slight increase of thermal degradation temperature (Eom, Kim et al. 2011). Asadieraghi et al. attributed the increase in thermal degradation temperature of biomass less in minerals to the reduced catalytic reactions as a result of mineral reduction (Asadieraghi and Daud 2014). Similar findings were made by Aslam et al. who studied the effect of acid washing of biomass, where they concluded that reduction in minerals leads to improved thermal degradation temperature due to reduced catalytic activity (Aslam, Ramzan et al. 2016). They also found that sulfuric acid was more effective in removing minerals than hydrochloric acid and they reported an improvement in heating value (by 7.1% for rice husk) as a result of mineral reduction using acids (Aslam, Ramzan et al. 2016). Another study by Eom et al. where they observed the effect of K, Ca and Mg impregnated on pure cellulose revealed that only K has a catalytic effect on cellulose decomposition (Eom, Kim et al. 2012).

Minerals in biomass have adverse effects on bio-oil from fast pyrolysis in terms of its quality and quantity. In general, the bio-oil yields from woody biomasses are higher compared to that from herbaceous biomasses (Carpenter, Westover et al. 2014). Henrich et al. attributed this to the high ash content of herbaceous biomasses which may have caused secondary reactions and reduced the bio-oil yield (Henrich, Dahmen et al. 2016). Trendewicz et al. studied the effect of potassium on cellulose pyrolysis and found similar conclusions as above that mineral rich cellulose produced less oil and they attributed it as the result of catalyzed dehydration reactions, which increased the char and gas yields

(Trendewicz, Evans et al. 2015). Hwang et al. studied the fast pyrolysis of potassium impregnated poplar wood and found that the char yield increased by 2 times compared to demineralized sample at various reaction temperatures and also observed the increase in water content of bio-oil with decreased viscosity due to minerals (Hwang, Oh et al. 2013). Eom et al. studied the effect of pyrolysis reaction temperature on demineralized rice straw and found that as the bio-oil and char yield decreases as a result of rising pyrolysis reaction temperatures and concluded that higher temperatures with demineralized rice straw may have led to more gasification reactions (Eom, Kim et al. 2013). Choi et al. found that water washing of S. *japonica* have significantly increased the activation energy and pyrolysis conversion characteristics (Choi, Kim et al. 2017). Brown et al. studied several mineral removal pretreatment processes like acid hydrolysis, washing with dilute nitric acid etc. to improve the pyrolytic yield of levoglucosan from herbaceous feedstocks, and concluded that the most effective treatment was washing with nitric acid (Brown, Radlein et al. 2001). Oudenhoven et al. studied the effectiveness of using wood derived acid in demineralization of pine wood in improving levoglucosan and found that the yields were comparable to that of mineral acid washing (Oudenhoven, Westerhof et al. 2013). Liu et al. found that the presence of AAEM's increase the phenolic compounds yield during pyrolysis as a result from demethxylation and demethoxylation (Liu, Wang et al. 2017). Messina et al. found that demineralized sawdust from invasive species produces bio-oil with higher heating value and char with high specific surface area compared to untreated sawdust (Messina, Bonelli et al. 2016).

2.3.4 Thermal pretreatment for fractional pyrolysis

The bio-oil produced from raw biomass is unstable, corrosive, viscous and has high water content (Aubin and Roy 1990, Diebold 1999). The biomass has several different structural and non-structural components which have distinct properties, processing biomass feedstock on as is basis for bio-oil will create complex reactions with these components can create bio-oil with the above mentioned undesirable characteristics (Agblevor and Besler-Guran 2002).

Branca et al. studied effect of torrefaction conditions on fixed bed pyrolysis and found that including torrefaction as a pretreatment method improved desirable anhydrosugars, guaiacols (carbonyl group) and phenols, reduced the amount of undesirable compounds like acetic acid, formic acid, furfural and hydroxyacetaldehydes (Branca, Di Blasi et al. 2014). Zheng et al. studied the effect of torrefaction temperature on pyrolysis behavior of biomass concluded that two step pyrolysis of biomass decreases the bio-oil yield compared to single step pyrolysis, however the benefits of more phenolic compounds and less oxygenated compounds like organic acids outweigh the disadvantage of low oil yield (Zheng, Tao et al. 2017). Cai et al. found similar finding when they studied the two step pyrolysis of sawdust and rice husk (Cai, Fivga et al. 2017). Westerhof et al. studied stepwise fast pyrolysis of pine wood with torrefaction at different temperatures (260-360 ºC) and pyrolysis at temperature of 530 ºC; they found that the feedstocks which were torrefied below 290 ºC and then pyrolyzed at 530 ºC produced a cumulative liquid yield similar to the yield from single stage pyrolysis at 530 ºC. However, the feedstocks torrefied above 290 ºC have produced lower cumulative yield compared to single stage

pyrolysis indicating the importance of torrefaction temperature in two step pyrolysis (Westerhof, Brilman et al. 2012). Similar study by Zhou et al. releveled that high torrefaction temperatures (> 310 ºC) the formation of secondary reactions significantly reduce the amount of levoglucosan and enhance the char yield (Zhou, Liaw et al. 2014).

As the bio-oil yield benefits from both torrefaction and mineral removal, there had been several studies made on the concept of combining mineral reduction and torrefaction of biomass to get optimal bio-oil yields. Wigley et al. studied the integration of acid washing and torrefaction in fast pyrolysis process and observed an improvement of bio-oil yield, levoglucosan and oil stability, and reduction of undesirable compounds like water, organic acids, aldehydes, high molecular compounds, inorganics (Wigley, Yip et al. 2016, Wigley, Yip et al. 2016). Similar results were observed by Chen et al. who studied on integrating torrefaction liquor washing and torrefaction, in addition to observed increased phenolic species and improved heating value (Chen, Mei et al. 2016). Zhang et al. had also observed similar behavior, however they used simple water washing and torrefaction (Zhang, Dong et al. 2016). Klemetsrud et al. had studied the effect of acid washing of grass clippings and waste paper for fast pyrolysis and found significant improvement in levoglucosan levels and oil yields compared to processing untreated feedstock (Klemetsrud, Ukaew et al. 2016).

2.4 Conclusions and outcome from literature survey

From the extensive literature survey the impact of different pretreatment methods were analyzed. Several technological and knowledge gaps were identified.

The major hindrance of biomass derived fuel is its feedstock cost, variability and mineral content. Low cost feedstocks such as Ag-wastes and MSW have high mineral content which pose a major challenge in using them as viable feedstock for fuel production. Many studies had proposed several techniques to reduce the mineral content of biomass ,however, long residence time, high water to biomass ratios and use of acids (both organic and mineral) will make these mineral reduction methods redundant and expensive for commercialization.

Bio-oils produced from raw biomass are unstable, viscous, and corrosive and high water content which effects its applications in diversified fields. Several studies had proven that by adopting multi-stage pyrolysis with the integration of torrefaction, mineral removal and catalysts can produce stable bio-oils which are less viscous and corrosive and have higher heating value. Modeling and techno-economic studies have shown positive results in terms of final fuel cost and GHG emissions by integrating torrefaction in pyrolysis process. These studies create a strong prospects for multi-stage pyrolysis integrating one or more pretreatment methods for optimal bio-oil production with lower upfront oil upgrading costs.

3 Experimental

3.1 Pretreatment methods

3.1.1 Mineral removal

It has been understood from the literature that the minerals (Alkali and Alkaline earth metals/AAEMs) embedded in the biomass are major hindrances for producing bio-energy related products. The traditional mineral removal methods/demineralization techniques such as leaching discussed in literature need pretreatment of raw biomass in terms of grinding and long soaking time of several hours to days. On the other hand, most of the leaching methods use acid as a powerful reagent to reduce the minerals. These parameters could become impracticable for commercial production of bio-fuels as they require a lot of energy for grinding raw biomass, lots of storage space for batch soaking, longer process times and corrosive effluent treatment. Current work focuses on reducing the impact of these parameters which would affect the future prospects of biomass derived fuels/bio-fuels.

A simple high shear mineral reduction technique was used in this work to be used to reduce the mineral content and size (to be discussed in following sections) of torrefied biomass. A custom built 5L stainless steel reactor with a high shear mixer from Charles Ross & Son Company (Model HSM-100LSK-1) was used to process all the demineralized samples used in this work (as seen in Figure 3.5). The RPM of the rotor can be adjusted from 500 to 10000 RPM. The primary purpose of this unit is to make a homogenous slurry of torrefied biomass with water. Both torrefied biomass and water are measured individually before processing and are added to the reactor. They are mixed at

a constant RPM for a specific time depending on the mineral reduction and comminution requirements. The final slurry is poured onto a filter/sieve to separate the solids (organic rich) from the liquid filtrate (inorganic rich). The separated products are weighed. The liquid filtrate samples are collected for further analysis for the composition of dissolved inorganic salts and the solid sample is dried to be used as a demineralized feedstock. The unit is capable of processing 500 grams of torrefied biomass at a given time.

3.1.2 Torrefaction

This work considers torrefaction as an important pretreatment method for raw biomass for producing quality bio-fuels. Torrefaction had been proved to improve many physical and fuel characteristics of biomass like grindability, hydrophobicity, heating value etc. This process weakens the fibers of biomass and assist in increasing the porosity of biomass; which helps in lowering the grinding energy and removal of lighter organic acids. The removal of these organic acids will be helpful in producing a good quality bio-oil with increased aromatics and has increased stability for storage and transportation. Reduction in acidic matter will be crucial in reducing the corrosion to the reactors and storage facilities in bio-refineries. The increment in the porosity will be helpful in mineral removal strategies which will be discussed in detail in the following sections.

A custom built stirrer/mixing paddle assisted steel batch torrefier was used in this work is shown in Figure 3.1. The rotational speed of the stirrer was fixed at 10 Hz with the help of a gear motor. The cylindrical shell is heated with six equally spaced 2 kW heaters. Temperatures of the stirred solids, produced gases and reactor shell were measured by type-K thermocouples. The reactor shell temperature was controlled by the feedback of

the solids temperature by using a SOLO (SL4824 series) temperature controller. The heating rate of biomass was measured at >2ºC/min. High purity nitrogen was continuously supplied into the reactor from the bottom to assist in inert atmosphere and drive the off-gases into the exhaust. Almost all of the samples were produced by heating the biomass to a target temperature and keeping the reactor at that temperature for 30 minutes before cooling it to the room temperature. Variety of torrefaction severities was the primary goal and was achieved by adjusting the temperature. The severity was quantified with the dry solids mass loss using weigh measurements. The replicate torrefaction experiments have provided an average mass loss with an error of 5-10%. However the severity/mass loss was hugely depended on the type of biomass, method timing and a few unknown varying system factors. Table 3.1 provides a classification of different severities with heating values based on torrefied woody biomass. This illustrated the relationship between mass loss and heating value. The mass loss of biomass corresponds to the loss of hydrogen and oxygen, which helps in increment of energy rich carbon content. The heating value can be increased with the mass loss i.e. reduced solids yield, however there should be a balance when considering the optimal parameters for efficient fuel heating value. In addition to the system mentioned above, torrefied biomass used in this work was also produced from using the fast pyrolysis system discussed in section 3.2.

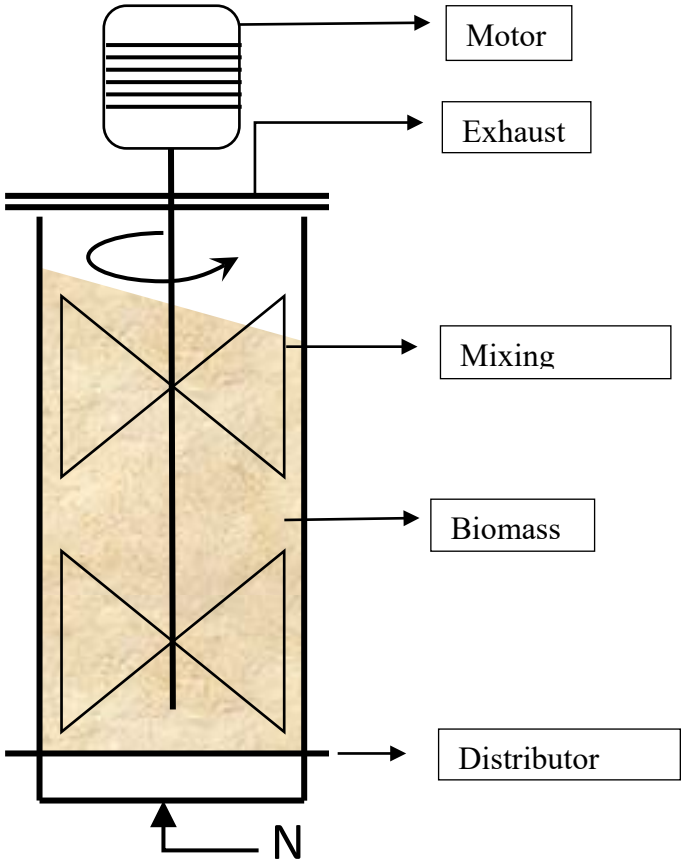

Figure 3.1 Schematic of continuously stirred batch torrefaction reactor (Donepudi, Zinchik et al. 2017)

Table 3.1 Torrefied biomass classification and approximate average heating value (Donepudi, Zinchik et al. 2017)

Classification Name	**Mass loss, %**	**Heat content, MJ/kg**
Raw biomass	0.0	19.1
Light brown	15-25%	20.7
Brown	25-40%	21.2
Dark brown	40-50%	22.3
Black	>50%	>23.3

3.1.3 Comminution

Comminution/size reduction is an important biomass pretreatment. Smaller particle sizes are always desirable in many bio-fuel processing plants, however it comes with a huge energy investment. As discussed in the literature, grinding raw biomass requires a lot of energy compared to treated/torrefied biomass.

In this work three size reduction grinders were studied for particle size distribution and energy. All the three grinders work on principle of shear forces and are specially chosen due to the fibrous nature of the biomasses studied. The first grinder is a batch type high speed rotor grinder by Col-Int Tech (Model FW-800) which can handle 800 grams of sample and operates at 24,000 RPM with the help of a 1.5 kW motor. The second grinder is a continuous type disc grinder by Modern Process Equipment (Model GP-140) which can handle a 50 kg/hr feed. However, due to subsequent processing and analysis needs, a fine sample was needed and the grinder was downgraded to handle only at a rate of 5 kg/hr. The third grinder was an aqueous high shear mixer/grinder by Charles Ross & Son Company (Model HSM-100LSK-1), which has an operating RPM with a range of 500-10,000 RPM. This grinder is different compared to other two traditional grinders, and is intended for wet-milling applications. It has been included in the work as it can multi perform as means of comminution and mineral reduction at the same time (detailed discussion in section 3.1.7).

The grinding energy from the grinders was measured using a power meter by Electronic Educational Devices (Model Watts-Up Pro 57777). This device/meter is connected in-line between the supply and grinder. The device is capable of measuring voltage and

current with a frequency of 1 Hz. Please note that the energy from grinder 2 was not considered for this work as it is an industrial grade grinder which runs on a 480 V, 3 phase supply and was used for only comparison purpose and more importantly it is a continuous type grinder compared to 1 and 3 which are batch type. The integration of the measured current gives the power consumption of the grinder. The baseline current consumption of the dry grinder (grinder 1) was obtained by measuring the current at no-load condition for a minimum of 3 minutes. However, for the wet grinder (grinder 3) the process was slightly changed. The baseline for wet grinder was obtained by running the rotor with allocated amount of water. This way the baseline of the wet grinder includes the power required to grind/agitate water, which then can be applied to find the power consumed by only the biomass sample.

3.1.3.1 Particle size distribution

The particle size distribution was obtained for both the cases of dry and wet sifting. Dry screening was performed with a mechanical sieve shaker with five sieves/screens (Fisher Scientific). Wet screening was performed with a four deck vibrating screening machine/Vibroscreen from Kason Corporation (Model K18-4-55). The sifting action comes from the vibrations caused by rotating a calibrated eccentric weight at the bottom with high speeds. As this is used for wet applications, all the screens and decks were all made out of 304 stainless steel. The screens on both the dry sifter and wet sifter are arrange in order to facilitate gravity induced particle size distribution.

A Weibull distribution as a function of probability density (eqn. 1) and cumulative distribution (eqn. 2) were used to help tabulate the size distributions. Please note that the

passing sieve size was assumed to represent the fraction and yield where the particle size are biased high for the sake of regressions. For example, particles passing through two screens with 150 and 75 micron pores sizes; the particles passing through 150 and which are retained on 75 are considered as particle size of 150 microns. This is the reason for slightly high skewed particle size distributions compared to techniques used. A non-linear regression was used to obtain fits through reduction (sum of squared error) between predicted and measured values. The residual value was in the range of 2-3%, however a single higher value was observed for corn stover sample at 4.7%, which might be because of its fibrous nature and/or problems with sifting high aspect ratio/low density particles. The size distribution fitting parameters are provided in Table 3.2.

$$f(l,\lambda,k) = \frac{k}{\lambda}\left(\frac{l}{\lambda}\right)^{k-1} e^{-\left(\frac{l}{\lambda}\right)^{k}} \qquad \text{Eqn. (1)}$$

$$\int f(l,\lambda,k) = 1 - e^{-\left(\frac{l}{\lambda}\right)^{k}} \qquad \text{Eqn. (2)}$$

Where l is the characteristic particle diameter (passing size), k is the fitting parameter that represent a shape factor and λ is a scaling factor.

Table 3.2 Size distribution fitting parameters for sawdust and coal (Donepudi, Zinchik et al. 2017)

Sample	**λ**	**k**
PRB Coal	53.0	0.89
Black	102.4	1.41
Dark Brown	170.7	2.25
Light Brown	267.2	4.20
Raw	458.8	1.88

3.1.4 Grinding energy

In this work size reduction and comminution energy were investigated using a high RPM rotor grinder and a disc grinder for comparison. The grinding energy/efficiency was measured using a range of torrefaction severities to observe its economic effect in the pre-processing stage.

From the results, it can be inferred that the power consumption peaked at the beginning and then followed a power-law type decay to an asymptotic value. The time value was assumed to be infinite to relate the power consumed by size reduced material with already ground material. A data acquisition system was used to continuously collect the voltage and current data from the power meter. The specific grinding energy can be obtained by plotting energy consumed as a function of mass through linear regression. Specific energy curves for several samples are shown in Figure 3.2. From the plot, the specific energy required for raw, torrefied-light, torrefied-dark brown are 4.9, 3.04 and 3.14 W/g respectively compared to 3.25 W/g of Powder River Basin/PRB coal. The intercept value for all the plots is almost same which represents the power required by the grinder at no-load. It can be illustrated that the power consumption decreases as the intensity of torrefaction increases and can reach the value for PRB coal. These values are comparable to the literature values (Phanphanich and Mani 2011). These results provide a strong basis for biomass pretreatment with torrefaction to reduce grinding costs with even a low torrefaction severity of 10-15% dry mass loss.

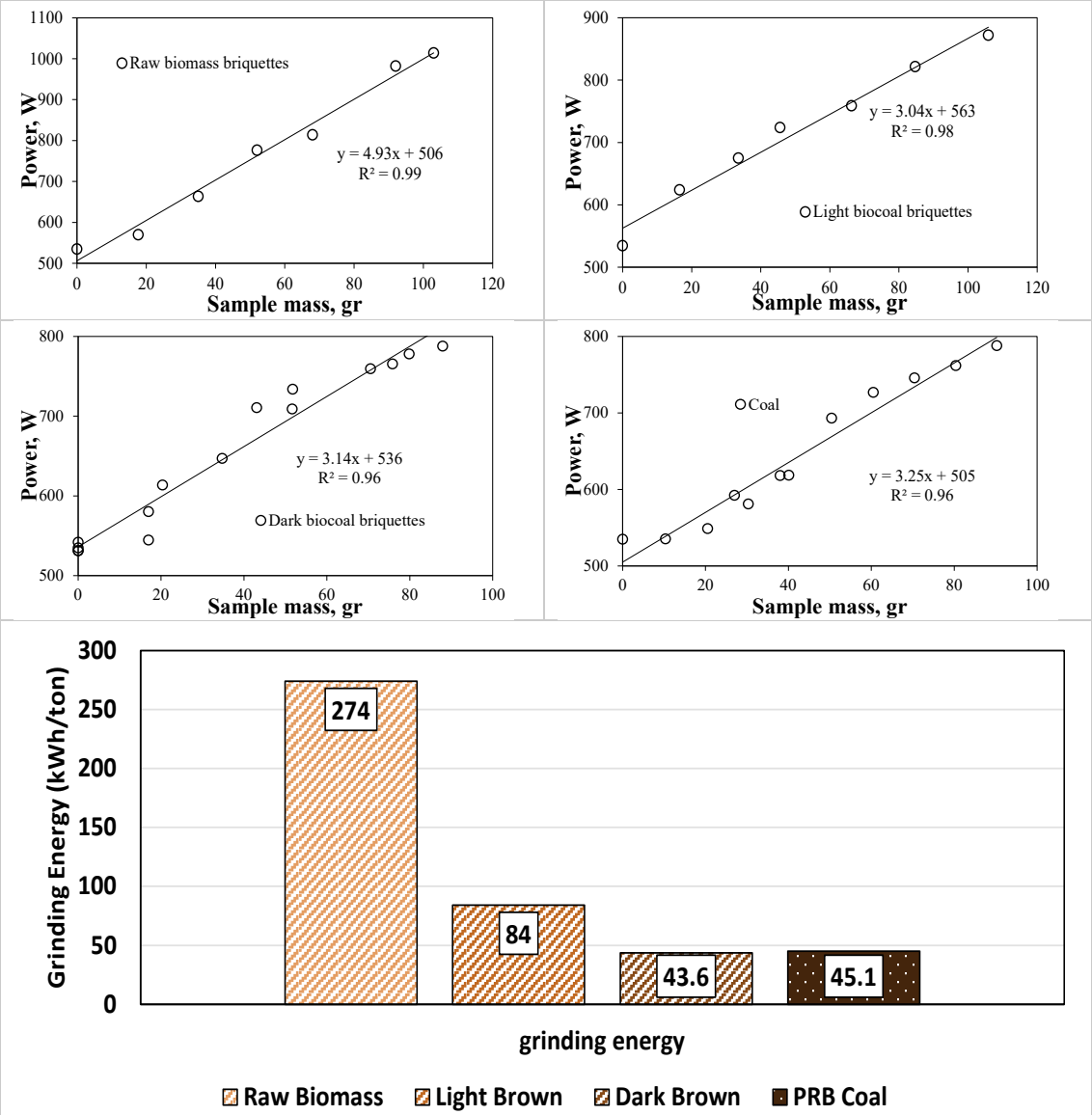

Figure 3.2 Grinding power consumption for raw sawdust, a reference coal sample, and two torrefied sawdust samples (Donepudi, Zinchik et al. 2017)

The summary of size distribution results of various samples can be seen in Figure 3.4.

3.1.5 SEM study

A scanning electron microscope (SEM) was used to image biomass (Arundo Donax/AD) fiber particles. Backscattered electrons were used to generate images on a solid state

backscattered detector. To minimize the damage and noise, the particles were gold coated. The results of SEM and Elemental Dispersive Spectroscopy (EDS) are shown in Figure 3.3. Scan (a) shows the particle scanned with approx. 10 AMUs which reveals mostly carbon and oxygen. Scan (b) shows a few silicon dioxide particles, which also appears on (d.1) and (e) in form of aggregates. However structural minerals like calcium and potassium seem to have been embedded into the fibers as seen in (c), (d.2) ad (f). The aggregate colonies, predominantly silicon dioxide appear to be in range of 2-10 μm and are loosely bound to the surface of the fibers. On other hand, the embedded structural minerals appear to be less than 2 μm. The SEM analysis showed an interesting approach towards ash content and size fractions of minerals associated with it. It also proves that minerals were part of the plant growth and not from external factors like harvest or wind.

The weaker association of insoluble minerals like SiO_2 to the biomass fibers and known minute size, make them a best candidate to start mineral separation with agitation, for example sifting. Several mechanical sifting experiments proved this phenomenon with AD and other feedstocks, where the ash content of the smaller size fractions was higher compared to larger size fractions which signify the removal of this type of minerals.

In the case of tightly bound structural minerals (mostly soluble), the agitation strategy did not work which indicates they might need a different treatment which includes dissolution of these minerals to reduce their content. This preliminary SEM study provided important findings in understanding the minerals in/on biomass fibers which will be used to formulate novel mineral reduction strategies which are discussed below.

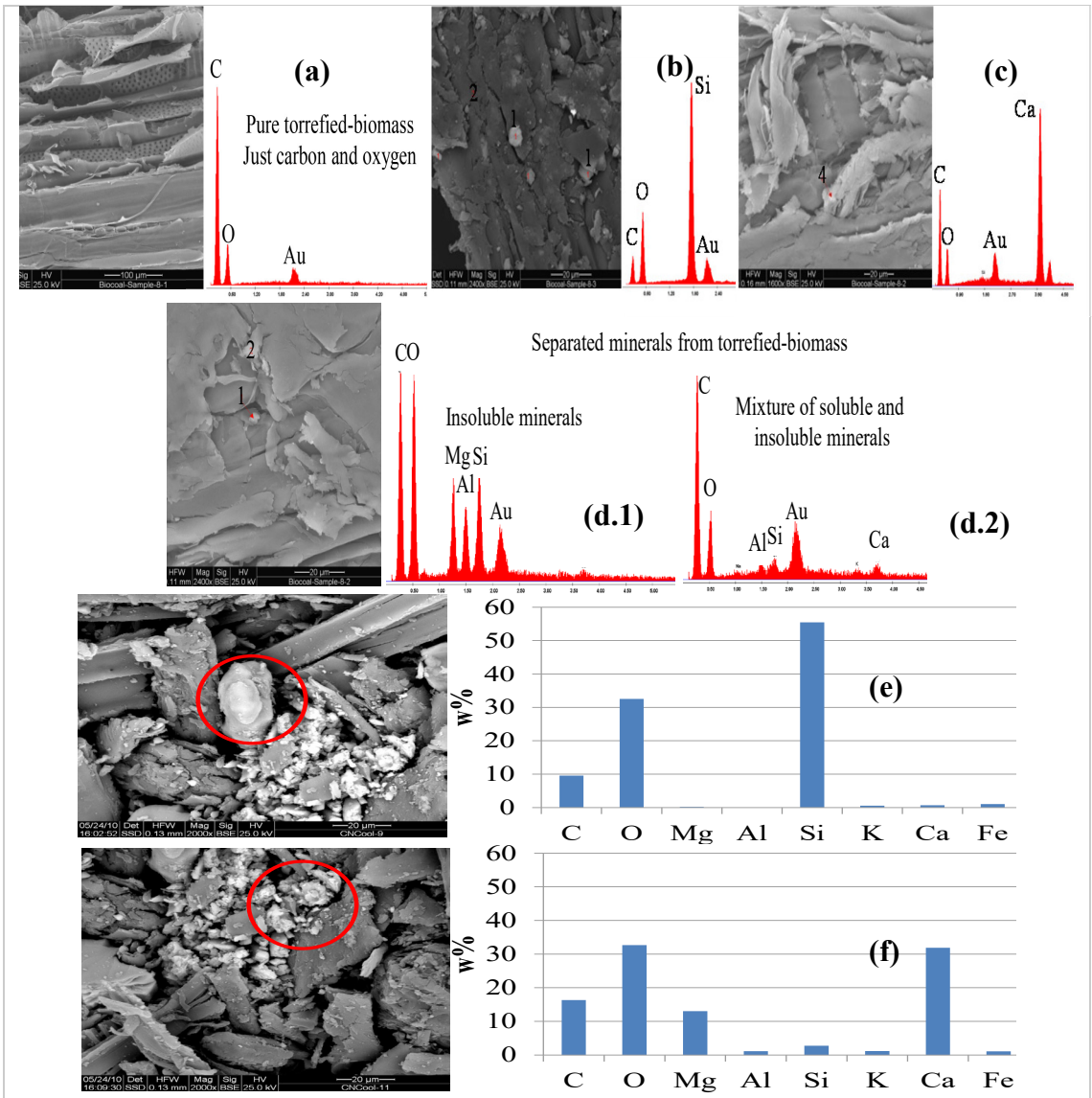

Figure 3.3 SEM and EDS of torrefied biomass fibers (Donepudi, Zinchik et al. 2017)

3.1.6 Dry Sifting

Sifting/dry sifting is one of the mineral reduction strategies explored in this work to remove any or all the loosely bound minerals from the biomass fibers. It was hypothesized that this weak associations would break with the agitation/vibratory forces through screening and would benefit the biomass with less ash content. A mechanical sieve shaker machine was used with tiered screens (Fisher Scientific) of pore sizes ranging from 850 to 45 microns.

Figure 3.4 shows the ash content results from sieving corn stover. Raw and torrefied corn stover with and without size reduction were investigated. However, raw corn stover without size reduction was excluded from the analysis as it did not pass through the largest screen. All the other three strategies (ground raw, ground torrefied and torrefied corn stover without size reduction) gave similar ash content results at different size distributions. From the results we can observe that the largest screen has material with lowest mineral content of original material (~12.5 wt%) and as the screen sizes reduced the ash content increased with the smallest screen having the largest amount of inorganics/ash at 60 wt%. As all the three strategies gave similar ash content results, it is crucial to consider how much material is retained on to different screens after sifting. Figure 3.4 (b) shows the fraction of ash (from combining the ash with the amount of material on the screen) with the size distribution which provides a clear distinction between different strategies. The ground raw corn stover and torrefied biomass without size reduction show similar behavior, where majority of the material retained on larger screens with high mineral content. However, the smaller screen with less material still

has a considerable amount of ash. From this result it is understood that even with high ash content in smaller screens, the majority of the material still has a lot of bound minerals on/within its fibers. This observation was inversed in the case of ground torrefied biomass, where it can be seen that most of the ash is in the smaller screens compared to the larger screen. It should be noted that once the material is ground, the amount of material retained in the smaller screens increases, which could also be observed in synchrony with high ash content on the plot for ground torrefied corn stover in Figure 3.4 (b).

These results stipulate that the three strategy technique of combining torrefaction, size reduction (grinding) and sifting can benefit the biomass by removing loosely bound (extractive/insoluble) minerals such as silicon. As discussed earlier, the dehydration effect of torrefaction will weaken the biomass fibers which will enable the release of these minerals during grinding compared to only sifting. It is speculated that the forces experienced by the biomass during grinding will help the removal of minerals bound to the fibers and size fractionation of this ground material will determine the amount of minerals removed with the amount of organics lost to the fines. This analysis does not quantify the dry sifting strategy, however it suggests that such method can be incorporated to remove minerals/inorganics while most of the organic matter is retained. The mineral reduction rate was improved with torrefaction, although it is unclear if this pretreatment assisted the loosening of minerals through increased porosity, swelling etc. or if the grinding was the prime driving force.

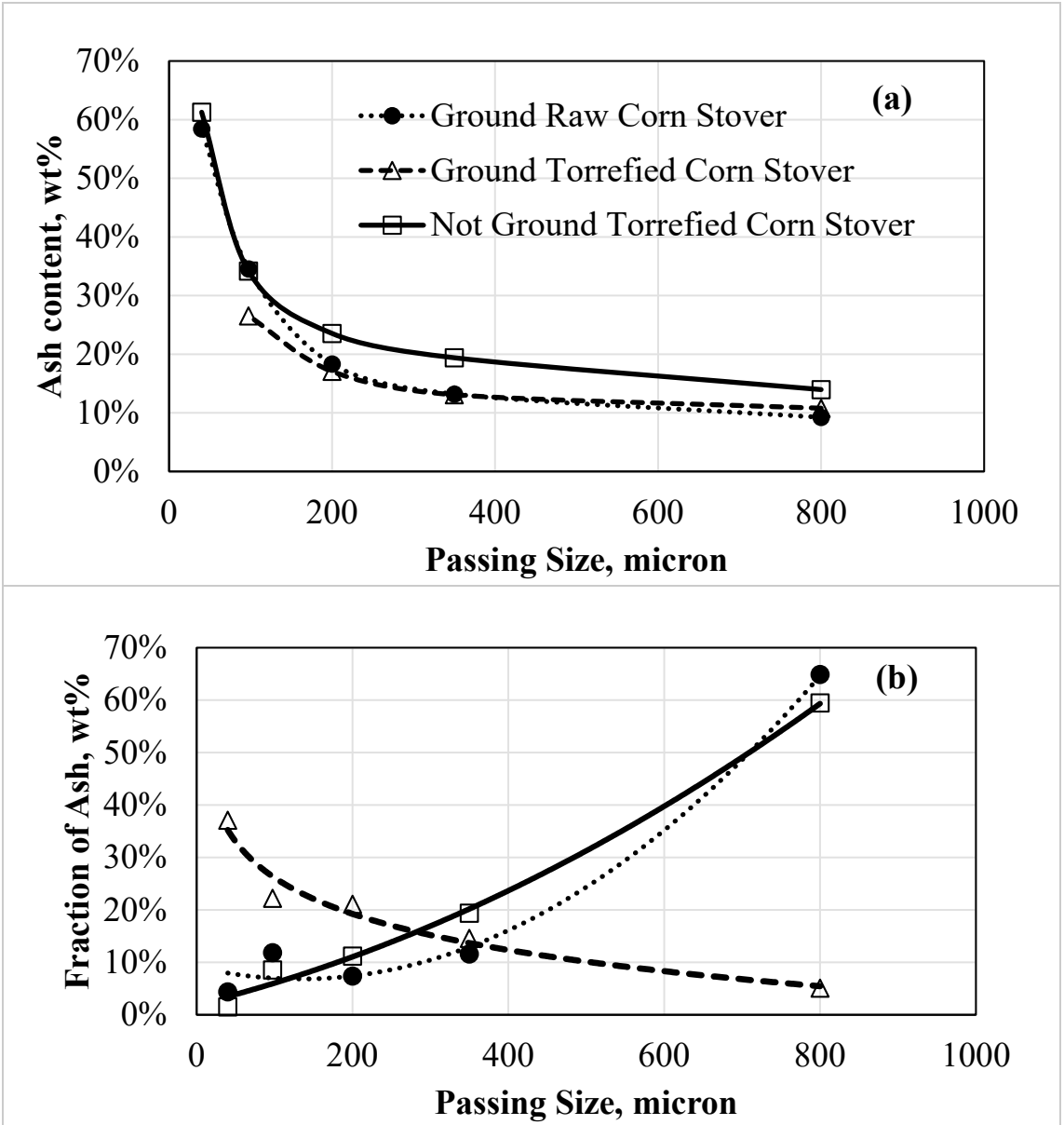

Figure 3.4 Dry fractionation of treated corn stover for inorganic reduction with (a) as measured ash content and (b) ash content in the whole sample (Donepudi, Zinchik et al. 2017)

3.1.7 Wet sifting and high shear mixing

A custom made setup used for wet sifting and high shear mixing can be seen in Figure 3.5. The setup includes a 5L stainless steel reactor with a high shear mixer placed on top of a tiered KASON vibroscreen machine (Model No. K18-4-55) (S-01 in Figure 3.5). Dry material is mixed with water to form a homogenous slurry using the high shear forces of the mixer. The residence time depends on the required mineral removal efficiency and final particle size, as this process is capable of multi performing. After a batch is processed for an allotted time, the slurry is released on to the vibroscreen by opening the valve V-01. Additional water is used to clean the reactor and promote solids flow off the screens on the vibroscreen machine. Solids and liquid fractions are collected and stored in sealed containers for further analysis.

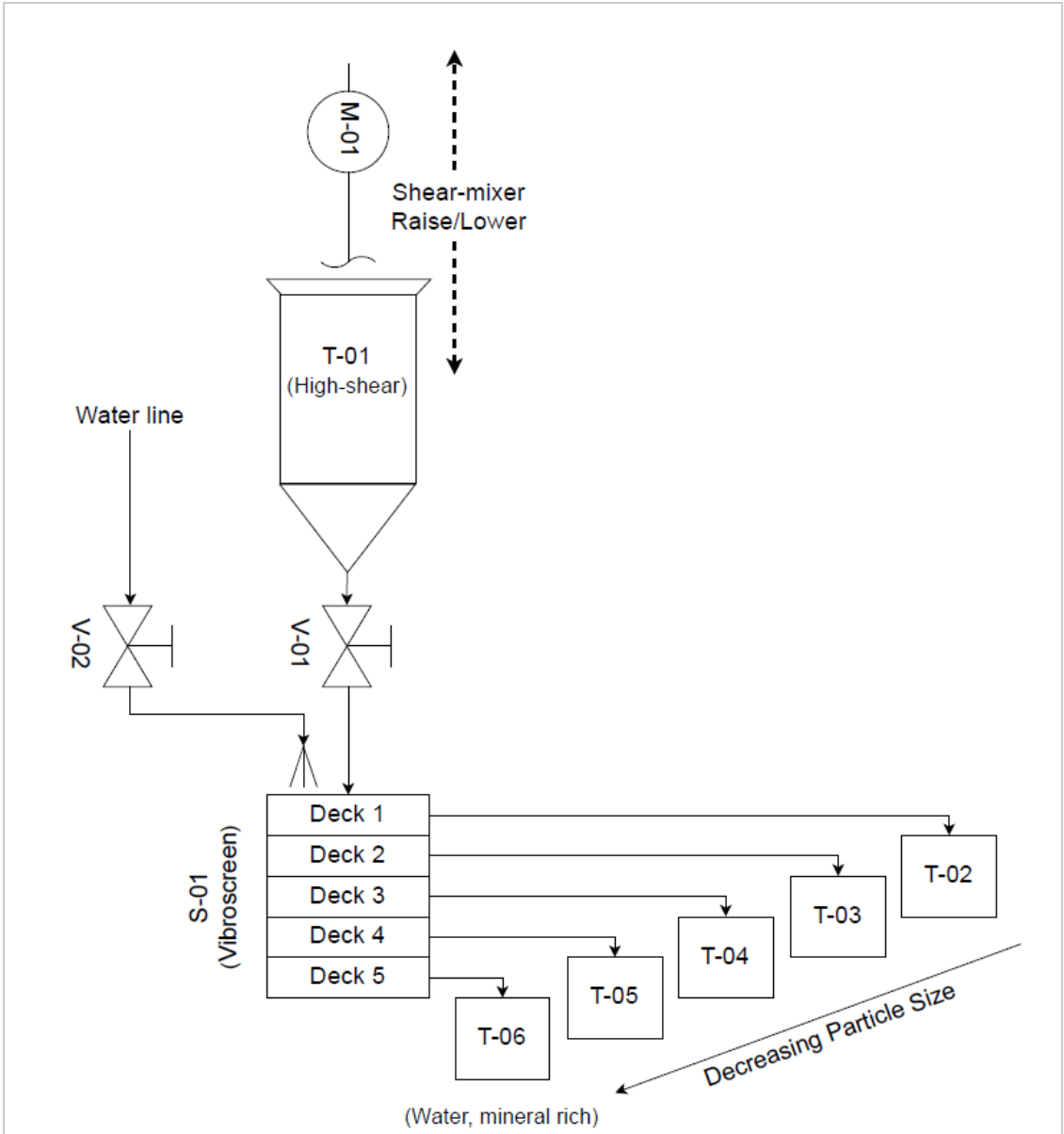

Figure 3.5 Flow diagram for the aqueous high-shear and wet sifting process (Donepudi, Zinchik et al. 2017)

3.2 Fast pyrolysis reactor

3.2.1 Reactor design and operation

The reactor was a custom made mixing paddle reactor built at Michigan Technological University in collaboration with Idaho National Laboratory. This was capable of achieving various levels of biomass thermal treatments ranging from drying, torrefaction to fast pyrolysis. The schematic of the reactor is shown in Figure 3.6.

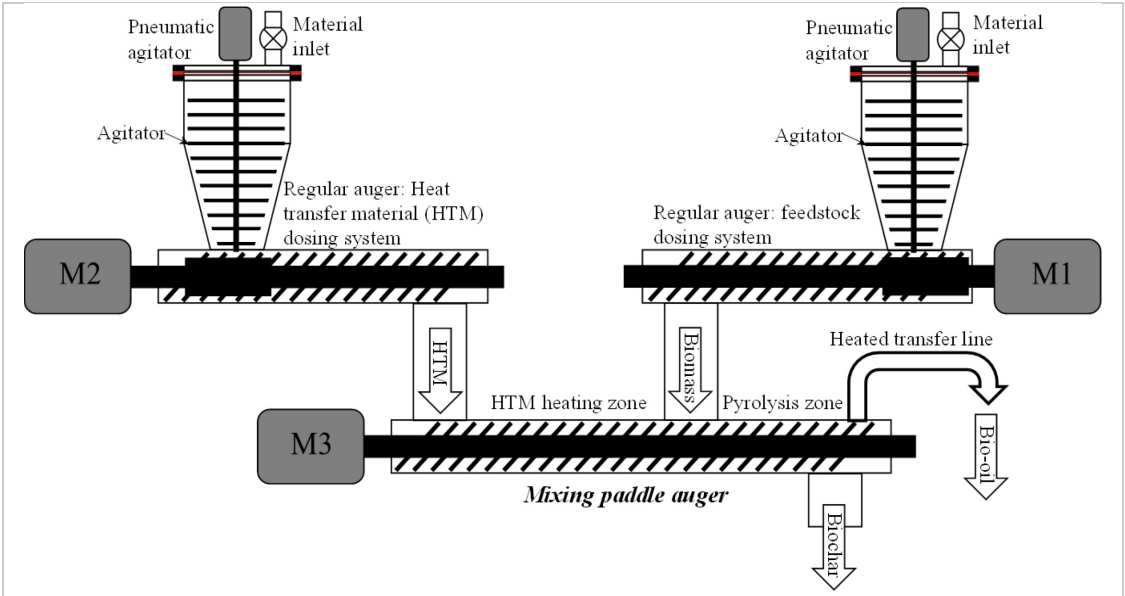

Figure 3.6 Process schematic showing major inlet/outlet streams from the pyrolysis reactor. (Zinchik, Klinger et al. 2017)

As seen from the Figure 3.6, the reactor consists of 3 major systems namely 1) Heat Transfer Medium (HTM) dosing system, 2) Biomass dosing system and 3) Reactor section with mixing paddles including product collection components. Both the dosing systems use regular screw type conveyors (commonly called augers). However, the reactor is a special auger with novel design which includes paddles formed by cut flights (Zinchik, Klinger et al. 2017). Detailed discussion of the reactor design and its characteristics are discussed in the following sections. It can be observed that both the

dosing augers are configured to be flood feeding type (with reduced pitch at the feeding section) and the rector auger is control fed type with constant pitch throughout its length. One more feature helping the uninterrupted flow of HTM and biomass are the agitators placed inside the hoppers which vibrate with a 50-100% of its rated duty by the help of pneumatic vibrators. Feed control is achieved by the three VFD (variable frequency drive) assisted electric motors attached to respective augers (namely M1, M2 and M3).

The reactor has several thermal regions. Both the dosing systems are exposed to room temperature/ without heating. The reactor is divided primarily into two regions, 1) HTM heating zone which brings the temperature of the HTM from ambient to the required target reaction temperature and 2) Pyrolysis zone where the HTM interacts with biomass at ambient condition and immediately transfers its thermal energy for the fuel conversion. The product spouts/transfer lines at the end of the rector are also heated. All the heated regions are heated with 1” ring heaters (1” width) placed throughout the heated length with thermocouples placed in between them, as seen in Figure 3.7. This will allow a tight control over temperatures to obtain optimal product.

The reactor is maintained air-tight with the help of graphite packing seals on all rotating parts and silicon/rubber seals for the vibrating parts. The entire reactor is purged with pure nitrogen during the experiment to encourage oxygen free environment and assist the flow of gaseous product out of the reactor into the collection system.

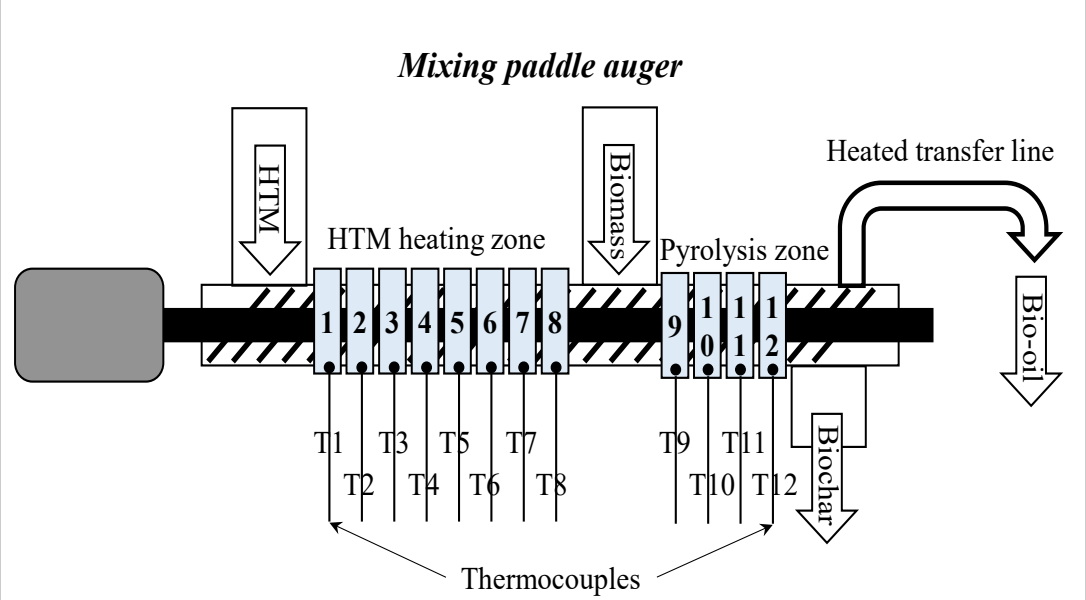

Figure 3.7 Heating of the mixing paddle reactor. (Zinchik, Klinger et al. 2017)

3.2.2 System overview and theory of operation

3.2.2.1 Dosing system

A similar dosing system was used for both HTM and biomass. The system is entirely made of 316 grade stainless steel. The dosing system has an inlet attached with a 3.5L (approx.) hopper, with gas grade valve and an agitator. The inner diameter of the dosing tube was 2.54 cm where the diameter of the auger shat was 1.27 cm. However, to reduce plugging of the material at the flood fed region of the auger the diameter of the shat was increased to 1.6 cm. The auger is rotated using a 3 phase VFD electric motor. The material at the discharge end of the dosing system is set to fall freely on to the reactor. Several experiments had concluded that a heated discharge section from the dosing system is recommended to have a plug free movement of material, especially for feedstocks with high moisture content.

3.2.2.2 Reactor features

The entire reactor section with paddle auger is made from 316 grade stainless steel. The inner diameter of the reactor tube is 2.54 cm. The diameter of the special mixing paddle auger is 2.54 cm with a shaft measuring at 1.27 cm. The pitch of the special auger is 5.08 cm. The auger had cut flights and paddles, each cut flight has five segments at 36º apart and there are four paddles angled at 45º to the shaft per each pitch, as seen on Figure 3.8. The cut flights help in creating inefficiencies in the flow which encourages mixing of already processed material with newly traversed material. The paddles help to move the material forward. This novel configuration had been proven to compete with leading fluid bed reactors in terms of yields, which will be discussed in the next chapter.

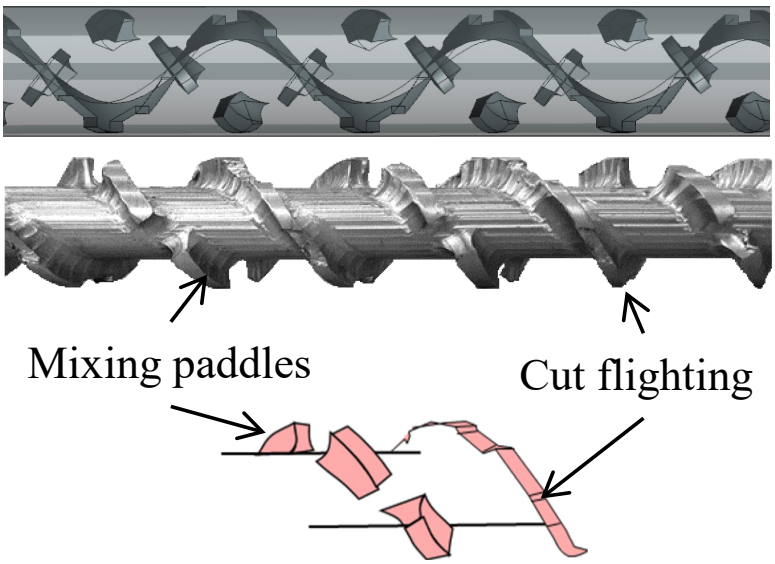

Figure 3.8 Top - 3-D model cutaway showing the mixing features of the auger reactor. Middle - photograph of the actual paddle reactor. Bottom - details of the cut flights and paddles. (Zinchik, Klinger et al. 2017)

3.2.2.3 Product collection

Fast pyrolysis of biomass results in solid and gaseous products. The solids are known as char (bio-char) and the gases/vapors contain condensable and non-condensable volatiles.

Bio-char included with HTM is collected through gravity by a sealed removable char collector vessel attached to the discharge end of the reactor. The char collector is uninsulated and left at ambient temperature to eliminate the possibility of char reactivity. The gases/vapors are carried to a shell and tube heat exchanger module through a heated transfer line with the help of inert nitrogen gas purging. The shell of the heat exchanger/condenser is chilled with continuous flow of water at 0 ºC, which will help the condensation of the condensable present in the gas stream into a thick liquor. This liquor is known as the bio-oil/pyrolysis oil which is collected into a HDPE grade bottle. At the discharge end of the condenser, there is an exhaust provision which will help the venting of remaining condensable gases/vapors into a simple water bubbling scrubber maintained at 0 ºC. After scrubbing, the non-condensable gases are vented to the stack/chimney.

3.2.2.4 Control system

The entire system is controlled with a central command center with the help of a human machine interface software (HMI) by Indusoft and programmable logic controller (PLC) by Automationdirect. The temperatures and duty cycles of the heaters are controlled by the PLC with the help of proportional-integral-derivative (PID) controller. The optimal PID parameters are obtained by extensive calibration tests and are representative of the heating rates of the material being used for processing.

3.2.2.5 Use of HTM

The use of a heat transfer material is crucial in fast pyrolysis as a rapid change in temperature of the biomass particle (delta T of 500 ºC) is required in less than a few

seconds. HTM also improves the homogenous thermal treatment of the biomass as it mixes through the length of the reactor interacting with the biomass particle on all sides. The main criteria for the selection of HTM is that it should have high heat capacity and should not react/influence as a catalyst within the chemical reactions occurring in the reactor. Other factors such as cost, ability of easy recovery and recycling and its effect of reactor in terms of wear and tear also influence the selection process. However, for the scale and type of use, washed sand (100-850 microns) was chosen for this work. The wear and tear of the sand on the reactor auger was evident at the laboratory scale and the special auger was replaced after 1000 hours of continuous work. However, this is impractical for large scale applications, and use of spherical HTM like stainless steel or ceramic shoots/balls are recommended. Recycling of certain HTM interacted with char is made possible by magnetic separation or mechanical separation through sifting.

3.2.3 Residence times

Residence time is one of the most important parameters affecting the yield and quality of the end product. The current system comprises of four important residence times; t_{HTM} for the HTM dosing auger, t_{bio} for the biomass dosing auger, t_{heat} for the heating section of the reactor and t_{pyr} for the pyrolysis zone of the reactor. The total residence time of the reactor is the sum of t_{heat} and t_{pyr}, see Eqn. (3). As discussed earlier the residence time is completely dependent on the rotational frequencies of the motors driving the shafts. The system has three motors for HTM, biomass and reactor sections respectively and their rotations are denoted as ν_{HTM}, ν_{bio} and $\nu_{reactor}$ respectively. The schematic in Figure 3.9 shows all the nomenclature used for different components of the system for residence

time calibration. A typical calibration experiment starts with feeding a measured amount of material (HTM or biomass) into the feeding section of the respective component (augers) and collected at the discharge section where its measured using a balance (readability of 0.01g). A data acquisition system was used to record the amount discharge per time. The rate of material discharge can be obtained from the slope of the graph plotted with weight vs time.

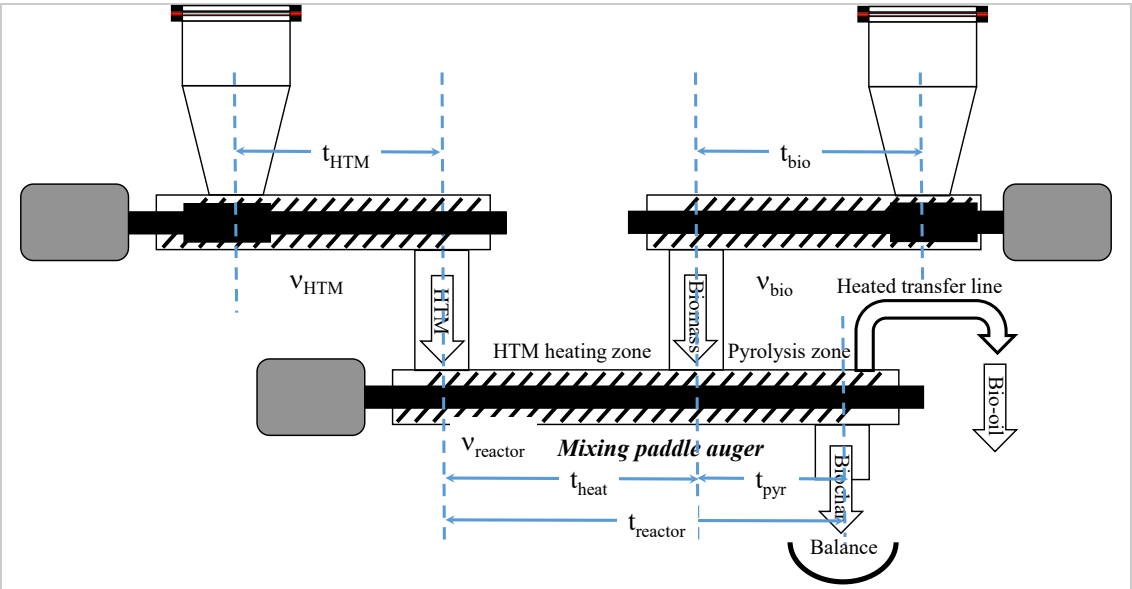

Figure 3.9 Residence time in each part of the system. (Zinchik, Klinger et al. 2017)

$$t_{reactor} = t_{heat} + t_{pyr} \qquad \text{Eqn. (3)}$$

3.2.3.1 Dosing augers

The two dosing systems use identical normal/standard augers (flood fed configuration). The residence time of the material flowing through these augers is given the correlation between rotational frequency (υ) and number of pitches on the auger (*c*), shown in Eqn. (4).

$$t_{residence} = \frac{c}{v} \qquad \text{Eqn. (4)}$$

Several calibration experiments were done on the system using sand (HTM) and various biomasses. Figure 3.10 shows one of such result, data from which t_{HTM} and t_{bio} (referred to as t_{tot}) are obtained with the flow rate of the material. Figure 3.11 shows a plot for residence times (HTM and biomass) vs one over constant reactor rotational frequency, from which rotation frequencies of HTM and biomass were obtained. As identical augers were used, the pitches for both the dosing augers were found to be identical at 5.72.

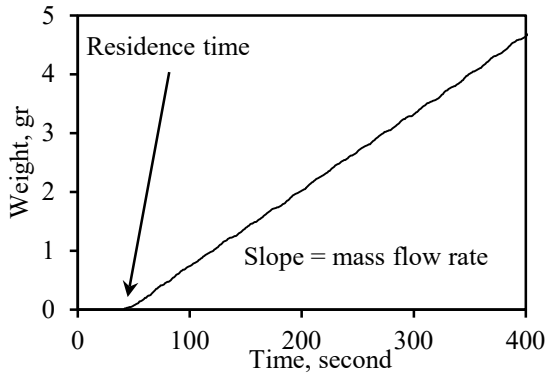

Figure 3.10 Biomass weight transients for determining t_{tot}. (Zinchik, Klinger et al. 2017)

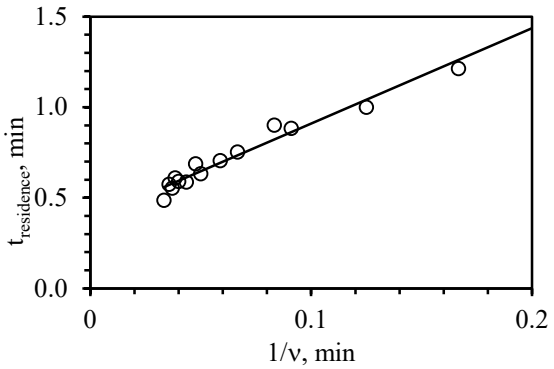

Figure 3.11 t_{tot} from biomass feed to reactor outlet vs. inverse biomass dosing frequency. (Zinchik, Klinger et al. 2017)

3.2.3.2 Novel mixing paddle auger

The calibration of the special auger used in reactor section is complex due to its design with cut flights and paddles. Therefore, correlation for normal augers showed in Eqn. (4) cannot be applied. For this reason, a new empirical correlation Eqn. (5) was made for the special auger with the help of material behavior inside the reactor and a few other assumptions. There are mainly three different components for the material movement inside the reactor with the special auger i.e. 1) forward push with axial component, 2) backward push and 3) sideway push by the radial component. On other hand, the residence time depends on percent filling of the material inside the reactor and the reactor rotation frequency.

$$t_{reactor} = \frac{c_{eff}(\nu_{reactor}, \nu_{HTM})}{\nu_{reactor}} \qquad \text{Eqn. (5)}$$

In the above equation, $c_{eff}(\nu_{reactor}, \nu_{HTM})$ is the effective number of pitches of the reactor that depend on the rotation frequencies of reactor and HTM and $t_{reactor}$ is the

residence time of the reactor. As both Eqns. (3.Y) and (3.Z) have similar parameters, a power-law model equation (Eqn. (6)) can be formed similar to them.

$$c_{eff}(\nu_{reactor}, \nu_{HTM}) = a_{reactor}\nu_{HTM}^{m}\nu_{reactor}^{n} \qquad \text{Eqn. (6)}$$

In the above equation, $a_{reactor}$ is a constant whereas m and n are the exponents for respective rotation frequencies. Substituting c_{eff} from Eqn. (6) in Eqn. (5) results in the following equation.

$$t_{reactor} = a_{reactor}\nu_{HTM}^{m}\nu_{reactor}^{n-1} \qquad \text{Eqn. (7)}$$

All the three parameters (*a*, *m*, and *n*) in the above equation are determined experimentally with a non-linear regression by measuring $t_{reactor}$ at different reactor and HTM rotation frequencies. The typical experiment is done with a filled HTM dosing auger and an empty reactor with a balance at the discharge that is capable of data acquisition to obtain the flow rate of the material from the reactor. The HTM dosing system and balance are stopped until the system is ready for the trial, meanwhile the reactor auger is turned on with a set frequency. Once the reactor auger reaches the set frequency, both HTM auger and balance are turned on and continuous mass flow rate data is gathered by the data acquisition system. Several experiments were done with varying reactor (20-200 RPM) and HTM (2-18 RPM) rotation frequencies. These results were then plotted with measured time vs calculated time using the Eqn. (3.B) which will obtain the values of the three parameters (*a*, *m*, and *n*), as shown in Figure 3.12. Eqn. (8) shows the complete equation for effective pitches (from Eqn. (6)) with empirical parameters.

$$c_{reactor}(\nu_{reactor}, \nu_{HTM}) = 9.68\nu_{HTM}^{-0.25}\nu_{reactor}^{0.5} \quad \text{Eqn. (8)}$$

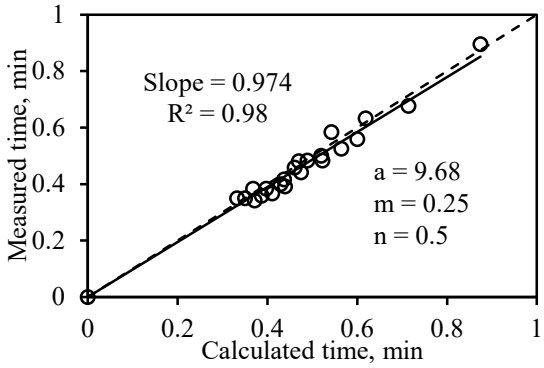

Figure 3.12 Measured $t_{reactor}$ vs. calculated time by Eqn. 7 (Zinchik, Klinger et al. 2017)

Figure 3.13 shows different c_{eff} values for different reactor and HTM rotation frequencies. The effective pitches can be a proportional parameter to determine the efficiency of mixing and thereby heat transfer rates. Eqn. (9) shows a new parameter p (pitch number) which can be representative of the mixing quality.

$$p = c_{eff}(\nu_{reactor}, \nu_{HTM})/c_{actual} \quad \text{Eqn. (9)}$$

Where, c_{actual} is the actual number of pitches on the special auger. By substituting the c_{eff} from the above equation in Eqn. (6), the new resultant p value is as follows.

$$p = a\nu_{HTM}^{m}\nu_{reactor}^{n-1}/c_{actual} \quad \text{Eqn. (10)}$$

Figure 3.14 shows different c_{eff}/c_{actual} values for different reactor and HTM rotation frequencies similar to the data shown in Figure 3.13, with the only difference being the

addition of c_{actual} which is 9 for the special auger. From these figures it can be observed that the c_{eff} ranges from 33 to 104 and p from 3.7 to 1.2, both corresponding to range of rotation frequencies of HTM from 3-18 RPM and reactor from 50-200 RPM. The quality of mixing increases with pitch number, p. The pitch number can also be seen as an indicator of the equivalent axial length and time spent the solid particles in a regular auger at similar rotation frequency; which means that the solid particles in the special auger can have the same effective mixing quality with less axial length and time compared to a regular auger. This will assist in reduction of the system footprint per unit of fuel produced.

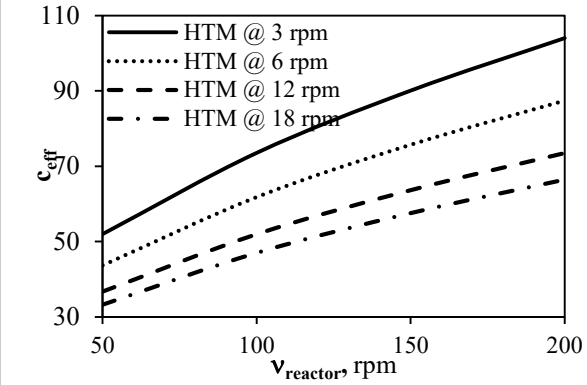

Figure 3.13 c_{eff} vs. reactor shaft rotation frequency. (Zinchik, Klinger et al. 2017)

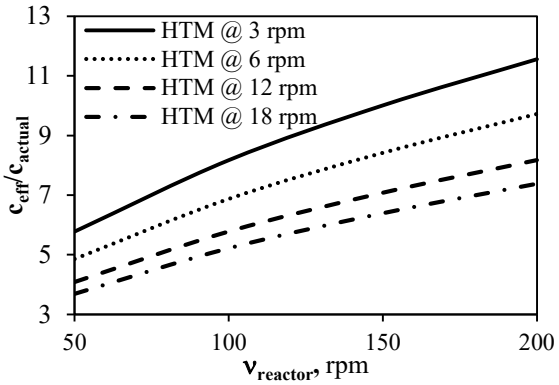

Figure 3.14 c_{eff}/c_{actual} vs. reactor shaft rotation frequency. (Zinchik, Klinger et al. 2017)

A similar analysis done on the pyrolysis zone of the reactor section yielded an effective number of pitches for that zone represented in Eqn. (11).

$$c_{pyr}(\nu_{reactor}, \nu_{HTM}) = 3.67\nu_{bio}^{-0.25}\nu_{reactor}^{0.5} \qquad \text{Eqn. (11)}$$

The ratio between the effective number of pitches of the reactor and pyrolysis zone is 2.67 which is rather close to the ratio of lengths of the reactor and pyrolysis zone of 3.0; this represents a linear relation between the reactor residence time with its length. Figure 3.15 shows the linear plot for measured residence time of reactor and pyrolysis zones vs calculated time.

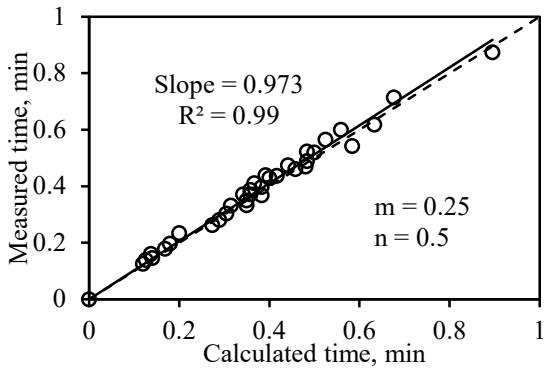

Figure 3.15 Measured residence time in the entire reactor and pyrolysis zone vs. calculated time. (Zinchik, Klinger et al. 2017)

3.2.4 Experimental methods

3.2.4.1 Material flow rates

A similar set up used in the residence time experiments discussed above (Figure 3.9), can be used to find the material flow rates. Figure 3.16 shows the typical experimental result from such calibration done using biomass, where its weight is represented with the discharge time. Figure 3.16 (a) shows the raw data with a slope of 0.788 g/min and Figure 3.16 (b) represents an instantaneous slope (periodic behavior as a result of auger operation with several pitches) taken for the same experiment which give a slope of 0.789 g/min. This proves that the rotation frequency is proportional to the material flow rate.

The major factors effecting the material flow rate are density and several physical characteristics like moisture content, size etc. For this reason the material flow rate calibration needs to be done on an individual basis for each and every biomass used for the experiments. For reference; Figure 3.I (a) shows the material flow rate for HTM (sand) and Figure 3.I (b) shows the material flow rate for sawdust. On an average the mass flow rate of HTM is recorded at 412 g/h per RPM and biomass is recorded at mere

41.7 g/h per RPM. This illustrates the importance of material density in accordance with its mass flow rate.

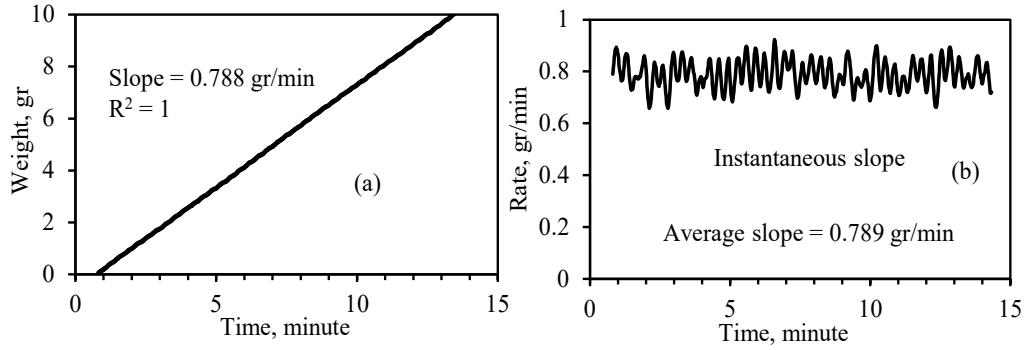

Figure 3.16 Typical weight transients of biomass (a) and instantaneous calculated rates (b). (Zinchik, Klinger et al. 2017)

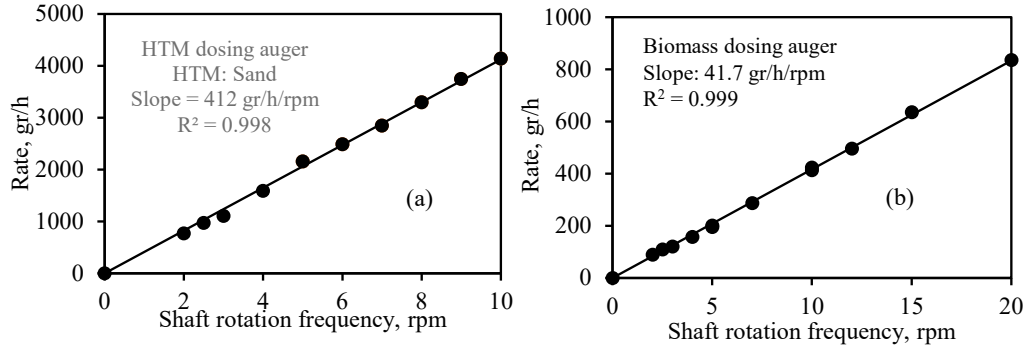

Figure 3.17 Calibration of the HTM - silica sand - dosing system (a) and the biomass dosing system for mixed hardwood sawdust (b). (Zinchik, Klinger et al. 2017)

3.2.4.2 Temperature set points and profiles

For fast pyrolysis experiments with an aim to achieve optimum oil yield to compare with the literature results, a fixed temperature set point is selected for HTM heating zone from T1 to T8 of 550 ºC to control the corresponding heaters 1-8 (as seen in Figure 3.7) and similarly for the pyrolysis zone the set point was 500 ºC from T9 to T12 to control the corresponding heaters 9-12 (as seen in Figure 3.7). Table 3.3 shows the data from a typical fast pyrolysis experiment of all the set points of all the heaters and corresponding

temperature reading at different stages of the process i.e. no load/ no material, with HTM and with HTM + biomass. From the data it can be observed that there was an excellent temperature control and the stability was around $\pm$0.1 ºC for almost all of the heaters.

Table 3.3 Temperature set-points and stabilized temperatures at various stages of operation. (Zinchik, Klinger et al. 2017)

	Set-point (°C)	**Empty System (°C)**	**With HTM (°C)**	**HTM and biomass (°C)**
T1	550	550.0±0.1	550.4±1.0	550.2±0.9
T2	550	558.4±0.1	557.3±0.5	556.5±0.4
T3	550	550.0±0.1	550.4±0.3	550.0±0.1
T4	550	550.0±0.2	550.3±0.4	549.9±0.2
T5	550	550.0±0.3	550.3±0.6	550.0±0.2
T6	550	558.0±0.1	555.0±0.5	558.3±0.1
T7	550	573.5±0.1	562.0±0.4	575.6±0.1
T8	550	550.0±0.1	550.3±0.4	549.9±1.4
T9	500	500.0±0.1	514.6±0.5	500.0±1.6
T10	500	500.0±0.1	500.4±0.3	500.2±0.5
T11	500	498.6±0.1	494.2±0.2	496.5±0.3
T12	500	500.0±0.1	500.2±0.1	500.1±0.1

Studying duty cycles of individual heaters can provide a better understanding of heating behavior and the heating requirements at different regions of the reactor section. Figure 3.18 shows the duty cycles of all the 12 heaters for an experiment at a given point of time when the system is producing bio-oil (the case of HTM + biomass). Here, the largest duty cycle was recorded by heater 1, which is obvious knowing that this heater is set at 550 ºC and is the first heater interacting with HTM (sand) at ambient condition. The large delta T between HTM and reactor core leads to large duty cycle of the heater. However, heaters 2 to 7 record negligible (almost zero) duty cycles, which shows that the HTM has reached its set/target temperature (550 ºC) by the time it leaves the heater 1 region. A considerable increase in duty cycle from zero can be observed in between heater 8 and 9. From Figure 3.7, this is the exact region where the biomass at ambient condition enters the hot reactor zone. However, the raise in duty cycle is very low compared to the heater

1 duty cycle heating the cold HTM. The main reason for this behavior is that the HTM is already hot and with its high heat capacity it raised the temperature of cold biomass instantly, reducing the load on heaters 8 and 9. After heater 9 the similar behavior can be observed, where the rest of the heaters show negligible duty cycle as the material (HTM + biomass) reached its set/target temperature (500 ºC) as it leaves the heater 9 region.

The most important part of fast pyrolysis is the biomass heating rate. Using the Gaussian distribution, it can be inferred that the biomass is fully heated after heater 9. The heating rate of biomass can be calculated by using the length of the heating zone and rotation frequency of the reactor. The length from the zone in between heater 8 and 9 and the end of heater 9 is measured to be approx. 3.2 cm. From the residence time analysis, this length can be converted to time, which is 4.3 seconds; which 0.73 cm/sec derived from the reactor's rotational frequency of 50 RPM (a calibrated frequency for all the fast pyrolysis experiments in this work). This will result in the approximate heating rate of 110 ºC/s (to increase the temperature of biomass from ambient to 500 ºC), which is superior to the standard past pyrolysis rate of 15-20 ºC/s. More detailed validation of the system parameters to perform fast pyrolysis is discussed in the following sections.

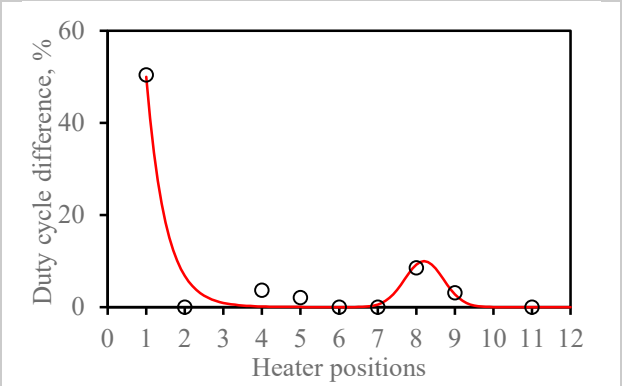

Figure 3.18 Difference between final and initial duty-cycles for each heater (after reaching steady state operation. (Zinchik, Klinger et al. 2017)

3.2.5 Thermal analysis and heating rate requirement

A heat transfer model was developed by Zinchik et al. at Michigan Technological University with the help of experimental data to study the thermal behavior of the current fast pyrolysis system and thereby understand the heating rate requirements. The two major assumption made were, 1) there is only axial heat transfer and 2) the material flowing through the system is assumed to be in continuum phase. (Zinchik, Ullal et al. 2017)

The heat transfer equation for the mixing paddle reactor is as follows;

$$\dot{q}(\dot{m}, T, x) = h(\dot{m}, T)A\Delta T + \dot{m}\int_{T_1}^{T_2} c_P(T)dT \qquad \text{Eqn. (12)}$$

Where,

$\dot{q}$ is the heating rate to raise the temperature of the material from T_1 to T_2 ,

A is the cross section area of the reactor, $\dot{m}$ is the material mass flow rate,

c_p is the specific heat capacity of the material,

T is the absolute temperature in K,

h is the heat transfer coefficient.

A typical experimental data of thermal gradient vs heating rate of different heating zones (see Figure 3.7) used for the modeling is shown in Figure 3.19. For simplicity purpose, first 10 heaters are chosen and were divided equally to become two zones 1 and 2 with different temperatures and the same nomenclature is used throughout the sections dealing with thermal analysis of the system (here in Figure 3.K the delta T was 50 ºC, where heater 1 thru 5 are maintained at 50 ºC and heaters 6 thru 10 were maintained at 100 ºC). The set/target points are denoted with dashed lines, whereas the actual measurements axial delta T values were represented with solid lines.

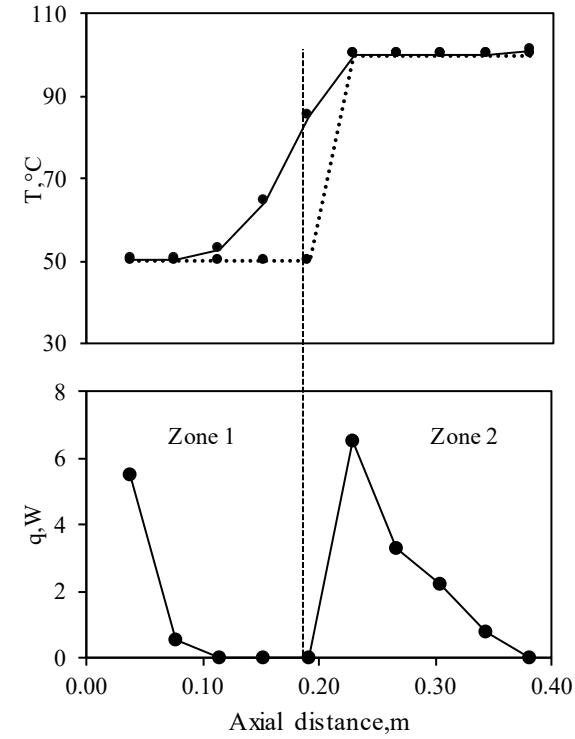

Figure 3.19 Typical set (dashed) and measured temperature gradient and heating rate of the paddle reactor. (Zinchik, Ullal et al. 2017)

3.2.5.1 Specific heat capacity

The specific heat capacities of sand (HTM) and biomass were measured for a variety of flow rates and temperature conditions (delta T's) as seen in Figures 3.20 and 3.21. The first five heaters (1 to 5) are maintained at the lowest temperature set points and the rest (6 to 10) were maintained at the highest temperature set points. To simply the analysis, both heat of reaction and effects of changing biomass composition are lumped together to represent the heat capacity.

At thermal steady state Eqn. (12) can be simplified as follows,

$$\dot{q}(\dot{m}, T) = \dot{m} \int_{T_o}^{T_2} c_p(T) dT \qquad \text{Eqn. (13)}$$

Where,

T_o is the ambient temperature,

T_2 is the final set temperature (maintained in Zone 2 (heaters 6 to 10)).

As the specific heat of many materials correspond to the square root of the absolute temperature, it was assumed that the specific heat varies with temperature and is represented as $c_p = c\sqrt{T}$ (c is a constant). Substituting the c_p in Eqn. (13) results in the following equation where the temperature dependence on specific heat can be determined by fitting the constant.

$$\dot{q}(\dot{m}, T) = \dot{m}c\frac{2\left(T_1^{3/2} - T_o^{3/2}\right)}{3} \qquad \text{Eqn. (14)}$$

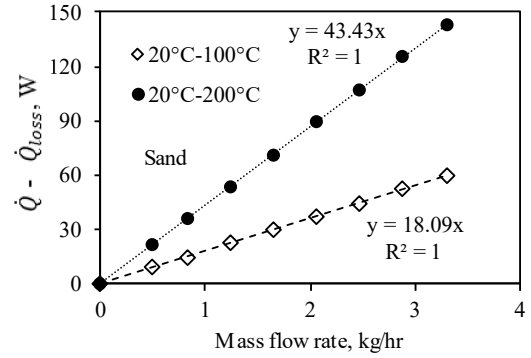

Figure 3.20 Net heating rate required to heat sand from ambient temperature to final temperature vs. mass flow rate. (Zinchik, Ullal et al. 2017)

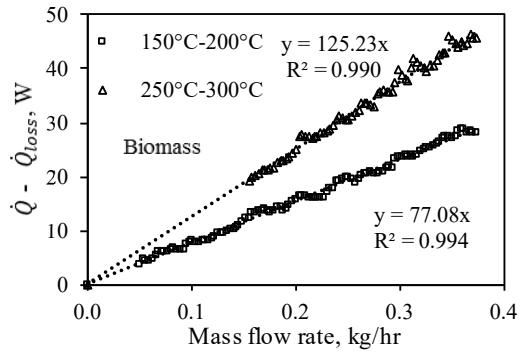

Figure 3.21 Net heating rate required to heat biomass from ambient temperature to final temperature vs. mass flow rate. (Zinchik, Ullal et al. 2017)

Using the data from several experiments and relating them with the above mentioned equations obtained the following specific heat correlations for sand and biomass with their respective c (proportional constant) values.

The correlation for sand is;

$$c_p(T) = 44.4\sqrt{T} \qquad \text{Eqn. (15)}$$

Similarly the correlation for biomass is;

$$c_p(T) = 78.8\sqrt{T} \qquad \text{Eqn. (16)}$$

The variation of specific heat of sand and biomass with temperature is shown in Figure 3.22. The sand plot has an overlay of standard specific heat values for quartz (similar to sand) from NIST (NIST), and it can be observed that the experimental correlation matches with the standard with high accuracy. Similarly for the values of specific heat of biomass are well in range published in the literature i.e. in between the range of 1300 to 2000 J/kgK (Dupont, Chiriac et al. 2014). The accuracy of the measured specific heat can also be illustrated by comparing the calculated and measured heat supplied to the system by simply substituting the specific heat values from Eqns. (15) and (16) in Eqn. (13) to obtain data for sand and biomass respectively. The results from this comparison are shown in Figure 3.23. It can be observed that both calculated and measured values agree with each other representing the accuracy of the found correlations for specific heat of sand and biomass.

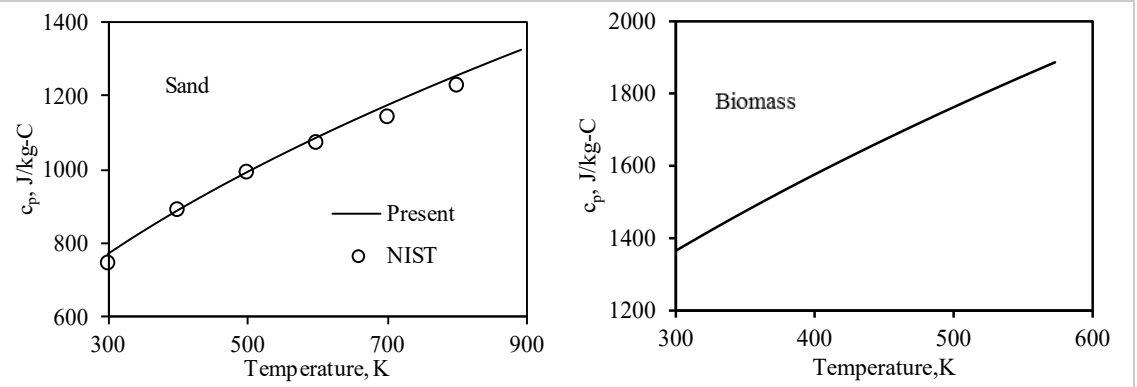

Figure 3.22 Specific heat capacity comparison (Zinchik, Ullal et al. 2017)

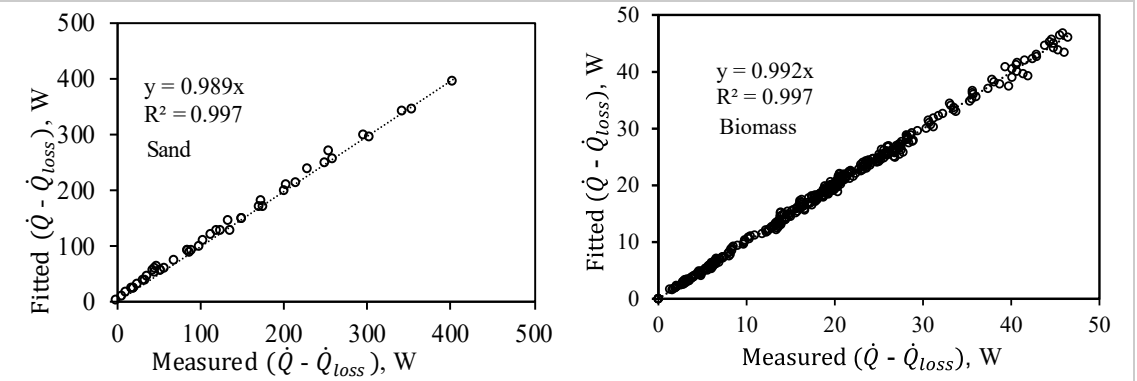

Figure 3.23 Fitted vs measured heating rates for sand and biomass (Zinchik, Ullal et al. 2017)

3.2.5.2 Effective thermal conductivity

Through several experiments it was observed that the heat transfer across the length (represented as $h\Delta x$, where Δx is the diameter of the reactor) of the reactor varies with the solid volume fraction ($\emptyset$) and temperature (T). The term $h\Delta x$ was assumed to represent the effective thermal conductivity (k_{eff}), which can be inferred as the axial heat transfer per unit area with a unit temperature gradient (Zinchik, Ullal et al. 2017). From the conclusions of the residence time experiments where it was observed that the mixing quality depends on the amount of material present in the reactor; it can be

hypothesized that the k_{eff} depends on solid filling fraction and absolute temperature and can be represented as follows,

$$k_{eff} \propto \emptyset^n T^m = A\emptyset^n T^m \qquad \text{Eqn. (17)}$$

Where,

n, m and A are constants,

$\emptyset$ is the solid filling fraction defined as the ratio of the volume occupied by the solid material particles (V_S) to that of the total reactor volume (V_R);

$$\emptyset = \frac{V_S}{V_R} \qquad \text{Eqn. (18)}$$

The volume of solid material particles can be represented by intrinsic density of the material (ρ_m), its residence time (t_{res}) and respective flow rate as follows,

$$V_s = \frac{\dot{m} t_{res}}{\rho_m} \qquad \text{Eqn. (19)}$$

It was assumed that the intrinsic density of the material only changes slightly with the degradation of biomass and was taken as a constant value. The residence time can be found by a correlation given below for biomass and sand derived from the residence time analysis (Zinchik, Klinger et al. 2017).

The correlation for the residence time for biomass flowing in the reactor at 200 RPM is as follows,

$$t_{res}(min) = 0.68(feed\ rpm)^{-0.25} \quad \text{Eqn. (20)}$$

Similarly, the correlation for the residence time for sand flowing in the reactor at 200 RPM is as follows,

$$t_{res}(min) = 0.83(feed\ rpm)^{-0.62} \quad \text{Eqn. (21)}$$

The properties of materials and constants used to obtain the above correlations are given in Table 3.4.

Table 3.4 Properties of materials

Quartz density (Haynes 2012)	2650 kg/m3
Wood density (Rabier, Temmerman et al. 2006)	1000 kg/m3
Reactor cross section area	0.000475 m2
Reactor volume	0.000214 m3

Two different heat balance equations can be represented for two different heating zones (as seen in Figure 3.19)

For Zone 1 (heaters 1 to 5) the heat balance equation is given as,

$$\dot{q}' + \dot{q}_1 = \dot{m} \int_{T_o}^{T_1} c_p dT \quad \text{Eqn. (22)}$$

Where,

$\dot{q}_1$ is the total heating rate of heaters 1-5,

$\dot{q}'$ is the heating rate conducting backward from zone 2,

T_o is the ambient temperature, and

T_1 is the first temperature step (lower temperature set point).

For Zone 2 (heaters 6 to 10) the heat balance equation is given as,

$$\dot{q}_2 = \dot{q}' + \dot{m} \int_{T_1}^{T_2} c_p dT \qquad \text{Eqn. (23)}$$

Where,

$\dot{q}_2$ is the total heating rate of heaters 6-10,

$\dot{q}'$ is the rate of heat leaving zone 2,

T_1 is the first temperature step (lower temperature set point),

T_2 is the second temperature step (higher temperature set point).

It was assumed that $\dot{q}_2$ assists in proving heat energy required to achieve the temperature gradient from T_1 to T_2 and is responsible for the heat loss from zone 2 represented by $\dot{q}'$.

Using the relation found for the effective thermal conductivity (Eqn. (17)), the Eqn. (23) can be rewritten as,

$$k_{eff} A \frac{\Delta T}{\Delta x} = \dot{m} \int_{T_1}^{T_2} c_p dT + \dot{q}' \qquad \text{Eqn. (24)}$$

From Eqn. (3.R) and Eqn. (3.S) the total heating rate of zone 2 ($\dot{q}_2$) can be represented as,

$$k_{eff} A \frac{\Delta T}{\Delta x} = \dot{q}_2 \qquad \text{Eqn. (25)}$$

The value of $\dot{q}_2$ can be determined from experiments. However, for biomass its value is obtained after deducting the heat for its moisture. The effective thermal conductivity can be given as (from Eqn. (25)),

$$k_{eff} = \frac{\dot{q}_2}{A} \frac{\Delta x}{\Delta T} \qquad \text{Eqn. (26)}$$

The effective thermal conductivities of sand and biomass were calculated using the above equation and were plotted against solid volume fraction of the material, shown in Figures 3.24 and 3.25.

Figure 3.O represents the data for sand/HTM. It can be observed that the effective conductivity is proportional to the volume fraction and temperature. However, temperature has very minor effect. From the residence time analysis it was proven that the solid volume fraction is always proportional to the mass flow rate, which infer with higher mass flow rates, there is increased heating load from the heaters which thereby increase the overall conductivity across the entire reactor cross section per given temperature gradient. The magnitude of increase in effective thermal conductivity is predominant for higher solid volume fractions. The non-liner regression of the Eqn. (3.L) with the data from this plot provides the k_{eff} correlation for sand (Eqn. (27))

$$k_{eff} = 11{,}464\emptyset^{3.64}T^{1.52} \qquad \text{Eqn. (27)}$$

Similar conclusions were drawn for the biomass data plotted on Figure 3.25 and the k_{eff} correlation for biomass is given by,

$$k_{eff} = 7{,}414\emptyset^{1.21}T^{0} \qquad \text{Eqn. (28)}$$

It can be observed from that biomass is less dependent on solid volume fraction compared to sand. From Figures 3.24 and 3.25, it can be seen that the effective thermal conductivities of the two materials gave similar magnitudes at temperatures below 300 ºC, with a volume fraction below 0.016 which is a good indication that the analysis was

consistent and the proposed effective thermal conductivity can be approximated to find the heat transfer of this complex system. The effective thermal conductivity is an empirically derived term ad should not be compared with the actual thermal conductivities of the respective materials.

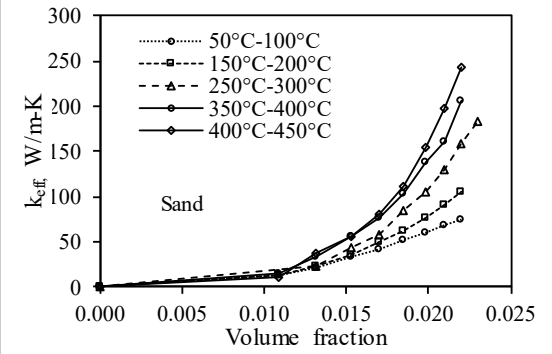

Figure 3.24 Effective thermal conductivity of sand, keff, vs. solid volume fraction in reactor at the temperature range 50°C-450°C. (Zinchik, Ullal et al. 2017)

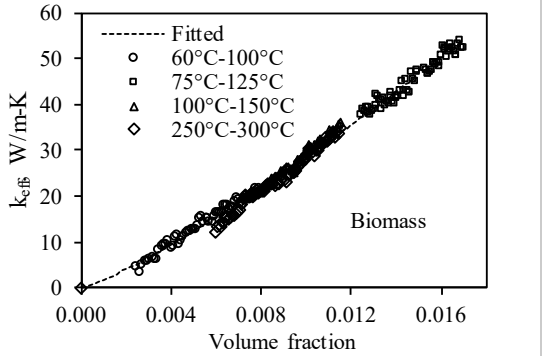

Figure 3.25 Effective thermal conductivity of biomass, keff vs. solid volume fraction in reactor at the temperature range 60°C-300°C. (Zinchik, Ullal et al. 2017)

3.2.6 Heating rates

High heating rates are needed for a proper fast pyrolysis. Heating rates have a predominant effect on the liquid yields (Di Blasi 1996). Following sections provide an insight on the investigation done by Ullal et al. on the effect of heating rates with and without the help of a heat transfer material (HTM) (Zinchik, Ullal et al. 2017).

3.2.6.1 With HTM

Optimal parameters like the HTM to biomass ratio (15:1) and rotational speeds of the dosing augers (controlled by motors M1 at 4 RPM for biomass and M2 at 6 RPM for sand/HTM (see Figure 3.6)) for the current system for proper fast pyrolysis are provided by Zinchik et al. (Zinchik, Klinger et al. 2017). These parameters were used in the one

dimensional model by Ullal et al. to find the transient temperature behavior (Zinchik, Ullal et al. 2017). All the thermal analysis parameter discussed in the sections above were found by using respective correlations. One important finding from the effective thermal conductivity analysis from the Figures 3.24 and 3.25 is that k_{eff} is more dependent on reactor compared to material. For this reason, it was proposed that the mixture k_{eff} (biomass + HTM) can be assumed as same as k_{eff} for sand and resulting solid volume fraction for this experiment will be 0.026.

The heating rate transient curve vs temperature as a result from the modeling are shown in Figures 3.26 and 3.27. With the help of HTM am instantaneous heating rate of 530 K/s was observed with a steady state temperature of 753 K (assume no losses). As the mass of sand is higher (15 times) than biomass, we observe only a slight change in its phase temperature.

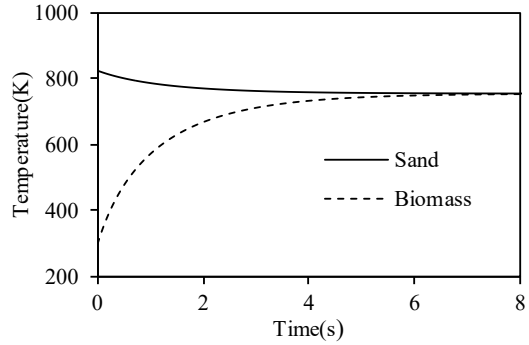

Figure 3.26 Temperature transient of fast pyrolysis of biomass (sawdust) with sand as HTM. (Zinchik, Ullal et al. 2017)

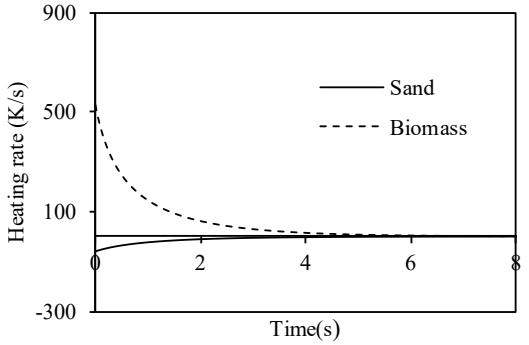

Figure 3.27 Heating rate transient for fast pyrolysis of biomass (sawdust) with sand as HTM. (Zinchik, Ullal et al. 2017)

3.2.6.2 Without HTM

To investigate the effect of not using HTM on the heating rate, a two zone experiment similar to the ones discussed in the previous sections was done by only using biomass

with set temperatures of 75 ºC for the zone one heater (1 to 5) and 125 ºC for zone 2 heaters (6 to 10). The resultant data from this experiment is shown in Figure 3.28.

To obtain heating rate, the spatial temperature gradient must be calculated. For the current system a sample gradient is shown below,

$$\frac{dT}{dx} \approx \frac{T_7 - T_6}{0.0254} \qquad \text{Eqn. (29)}$$

Where,

T_6 and T_7 are the temperature readings from thermocouples 6 and 7 respectively (see Figure 3.7)

0.0254 is the distance between the thermocouples which is equal to 2.54 cm or 0.0245 m.

This spatial temperature gradient can then be used in the Eqn. (26) to find the heating rate. From Figure 3.28 it can be observed that heating rate is directly proportional (linear) to the solid volume fraction. From the plot it is evident that heating rates exceeding 15 K/s can be achieved by only flowing biomass without HTM. According to Di Blasi et al., the threshold value of the heating rate to obtain maximum bio-oil yield from fast pyrolysis was 15 K/s (Di Blasi 1996), which means that by using the current reactor configuration, optimal bio-oil yield can be achieved by purely processing biomass without the need of HTM to assist higher heating rates. This is a significant discovery in this work as the primary HTM choice was sand which had caused many problems. Fast pyrolysis without HTM could have saving on costs, equipment wear/tear and elimination of hazards caused by fine silica dust.

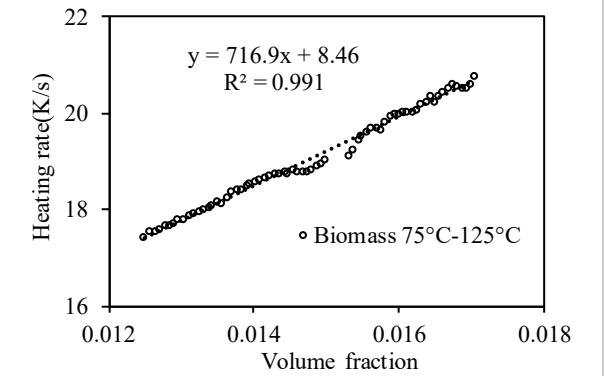

Figure 3.28 Heating rate vs solid volume fraction of biomass in the temperature range 75°C-125°C.

3.2.6.3 Validation of fast pyrolysis

From the above discussion it is evident that optimal heating rates for fast pyrolysis can be achieved without using HTM. However, the experiment was done using low temperatures (~125 ºC) which is far below any biomass thermal pretreatment condition. To have a proper validation of fast pyrolysis with the effect of HTM and other factors like minerals, the analysis should be doe from results obtained from different set of experiments using actual fast pyrolysis temperatures.

Table 3.5 shows the actual bio-oil yields obtained from fast pyrolysis experiments done with a single type of feedstock (i.e. forest residues) with varying parameters like pretreatments like torrefaction with 15% mass loss, demineralization, and use of HTM. From the experimental data for the torrefied biomass without HTM case, the average heating rate was 36 K/s which is above the literature threshold of 12 K/sec.

Table 3.5 Fast pyrolysis experimental results (Zinchik, Ullal et al. 2017)

Feedstock	**Liquid yield (%)**
Raw forest residues with HTM	55
Torrefied forest residues with HTM	44~46, 53 (demineralized)
Torrefied forest residues without HTM	50

These experimental results were compared with simulated/modeled results from a unified kinetic model for torrefaction-pyrolysis proposed by Klinger et al. (Klinger, Bar-Ziv et al. 2015). Figure 3.29 shows the results of liquid yields for various heating rates using the model. The unified model predicted a liquid yield of 66-67% (yield from both torrefaction and pyrolysis). The experiment with demineralized torrefied biomass yielded 53% liquid (pyrolysis only). However to compare the result with the predicted value, the liquid from torrefaction should be added to the experimental pyrolysis liquid yield. With 15% mass loss (dry basis) that the raw feedstock underwent during torrefaction to become torrefied biomass before it was used for fast pyrolysis, one can estimate 9-12% of the liquid might have been yielded through torrefaction. This number when added to the 53% pyrolysis yield from the experiment, the total unified liquid yield would become 62-65% liquid yield which comparable to the predicted value.

The small difference in predicted and actual yields might be from several factors. The model assume that the feedstock is 100% mineral/ash free, whereas the demineralized torrefied forest residue still have a few minerals in their fibers (as the ash content was 0.87%) which might have caused undesirable secondary reactions thereby reducing the yield. There might have been experimental errors, condenser and scrubber inefficiencies that might have caused the venting of condensable vapors/gases. Another factor might be the biomass composition might be different to that of the composition used in the model. Even with these many factors affecting the yield, the current system is capable of producing yields comparable to that of predicted values and mostly importantly the novel

reactor with mixing paddle configuration is capable of performing fast pyrolysis with similar yields without using HTM compared to the yields obtained from the use of HTM.

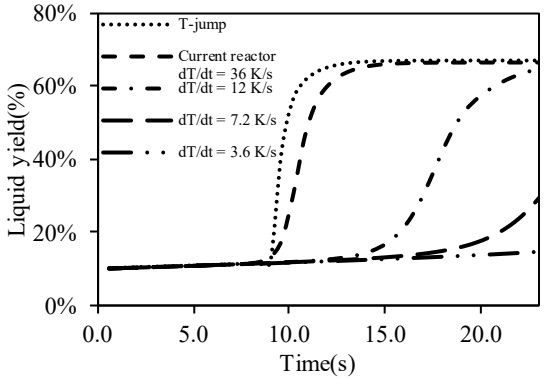

Figure 3.29 Liquid yield as predicted by the Klinger et al. model for various heating rates. (Zinchik, Ullal et al. 2017)

3.3 Fast Pyrolysis Processing

3.3.1 Mass balance during pyrolysis

Fast pyrolysis of biomass produces three products i.e. liquids (condensable), solids (char) and gases (non-condensable). The primary product of interest is the liquid fraction, commonly known as bio-oil. The yields of these three products depend on several factors and are predominantly influenced by feedstock, reaction temperature and rate of heat transfer. The reaction temperature can range from 470 º C to 530 ºC. However, most of the studies in literature proposed a mean temperature of 500 ºC as the optimal reaction temperature to obtain good oil yields for various feedstocks (Carpenter, Westover et al. 2014). Depending on feedstocks the oil yields can range from 34 to 68% (wt%), char yields from 10 to 35% (wt%) and gases 10 to 34% (wt%) (Carpenter, Westover et al. 2014). In general, woody biomass yield more bio-oil compared to herbaceous biomass due to lower mineral content (Carpenter, Westover et al. 2014).

3.3.2 Comparison to NREL results

The primary goal of the designed system was to demonstrate its ability to perform fast pyrolysis using a novel mixing paddle reactor. For this reason, a comparative study had been done using the char and bio-oil yields produced by NREL's fluidized bed reactor (known as 2FBR) (Westover, Phanphanich et al. 2013, Carpenter, Westover et al. 2014, Howe, Westover et al. 2015) compared to the yields produced by our mixing paddle reactor using ten similar feedstocks. Table 3.6 shows the set points used during the tests. The mass ratio of sand to biomass was chosen to be 15:1 which provided a particle ratio of 5:1 for their respective sizes, which is comparable to the values used in previous studies such as 18:1 (Brown and Brown 2012) and (Henrich, Dahmen et al. 2016, Pfitzer, Dahmen et al. 2016) 11:1. As the flow rate of sand and biomass change with their composition and physical characteristics like density and size the speed of the respective dosing augers were varied to provide approximately a similar feed rate for all the experiments. The speed of the sand dosing auger was set to provide a flow rate of 1500 g/h (approx.), whereas the biomass dosing auger was set to provide a flow rate of 100 g/h (approx.). The speed of the mixing paddles (reactor auger) was made constant for all the experiments.

Table 3.6 Set points for comparative study

Sand to Biomass mass ratio	15:1
Speed of HTM dosing auger	2.5-3 RPM
Speed of Biomass dosing auger	3-4 RPM
Speed of reactor	50 RPM
Conversion temperature	500 ºC

Figure 3.30 shows the results from this comparative study. Table 3.7 provides the details of char and bio-oil yields from various feedstocks tested. Thermally treated pine has

produced the highest amount of char of 33.2% and the lowest char yield was from hybrid poplar with 7.6%. The highest bio-oil yield was observed for tulip poplar (66.7%) and the lowest was from thermally treated pine (39.6%). In the Figure 3.30, the dashed line (with R^2=0.95) from the linear regression of the results with an intercept of 0.02 matched perfectly with the representative solid line (with slope=1), which confirms that the current system is capable of performing fast pyrolysis with similar product efficiencies from the literature. As discussed in the previous chapter, theoretically the system can perform fast pyrolysis without the use of HTM. To quantify the theory all the ten feedstocks used previously are processed without HTM and Figure 3.31 shows the results compared to NREL. Similar to the plot shown in Figure 3.30, the solid line in the Figure 3.31 is the representative of NREL results with a slope of 1, whereas the dashed line is the result of the linear regression of the results from experiments done without HTM with a slope of 0.64. This shows that fast pyrolysis without HTM will not result in equal yields when compared to the ones produced from using HTM at these operating conditions. The bio-oil yield reduction varied from 8-18% with respective to the yields from experiments using HTM. These tests conclude that even though the system is capable of performing fast pyrolysis without HTM, it must be optimized to match the superior product yields from the use of HTM through further improved geometry, mixing (reactor RPM), pre-heating or heat ramping, etc.

Table 3.7 Char and bio-oil yields from fast pyrolysis of various feedstocks

Feedstock	**Char yield (%)**	**Bio-oil yield (%)**
Switchgrass	19.7	64.8
Corn stover	8.6	56.8
Clean pine	10.8	64.6
Thermally treated pine	33.2	39.6
Blend*	13.2	58.5
Pinion-juniper	12.1	66.0
Tulip poplar	8.5	66.7
Hybrid poplar	7.6	61.6
C&D waste	11.3	59.6
Miscanthus	11.4	58.1
*- Consists of clean pine, tulip poplar, switchgrass		

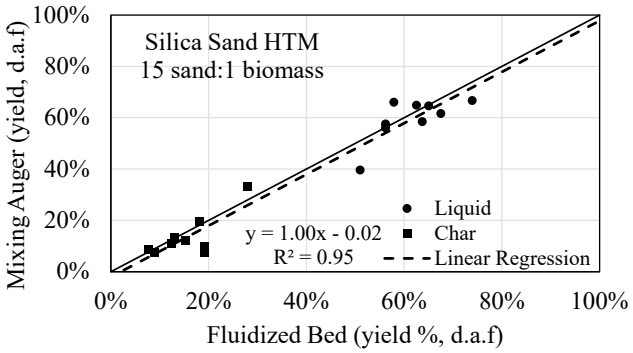

Figure 3.30 Plot of char and bio-oil yields vs. those of NREL for the same materials. The ratio between HTM and biomass was 15:1. (Zinchik, Klinger et al. 2017)

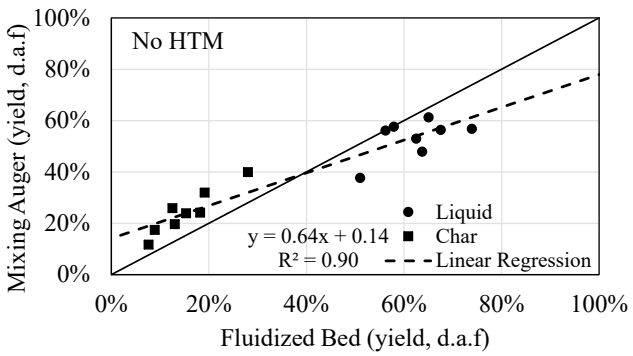

Figure 3.31 Plot of char and bio-oil yields vs. those of NREL for the same materials of Figure 14, without HTM. (Zinchik, Klinger et al. 2017)

4 Arundo donax

4.1 Parametric study with high-mineral Arundo Donax

The bio-oil yield from fast pyrolysis depend on various parameters such as conversion/reaction temperature, residence time, feedstock particle size, carrier gas flow rate, moisture content of the feedstock, etc. However, the two important parameters that have an impact on the liquid yield are conversion/reaction temperature and feedstock particle size, which are been chosen for this parametric study. The experiments to study the effect of reaction temperature were done with three temperatures i.e. 470 ºC, 500 ºC and 530 ºC on biomass with average particle size between 425 and 850 microns. The experiments to study the effect of particle size were done on three different particle sizes i.e. less than 425 microns, between 425-850 microns, and between 850-1000 microns using a reaction temperature of 500 ºC (Donepudi, Desai et al. 2017). The experimental matrix (with particle size, pyrolysis reaction temperatures and different pretreatment methods) used for this study is given in Table 4.1.

Arundo Donax (AD) was selected for this study for being a prominent energy crop with high biomass per sq. meter yield and faster growth. The feedstock received has a particle length of 4 inches with a width of approx. 0.25 inch. This feedstock is dried at 150 ºC using a forced air drying oven (Shel Lab SMO28-2) to a final moisture content of less than 5 wt%, measured by a moisture analyzer (DSC HFT 1000). The dried feedstock is then ground for 30 seconds using a rotor shear grinder (Col-Int Tech, FW-800). The ground feedstock is then sifted using No.18, No.20 and No.40 analytical sieves (Fisher Scientific) into four different fractions, and the largest fraction greater than 1000 microns

was discarded to be used in a different experiment. The ash content of all the three size fractioned samples were measured by using ASTM E1755-01 standard in a muffle furnace (Thermo Scientific, Lindberg Blue M). The ash content results are shown in the Table 4.2, where we can observe the concept that was discussed in Chapter 3 that the smallest size fraction (here it is less than 425 microns) has the highest mineral content. Sand as HTM was used for all the experiments for this parametric study to obtain maximum bio-oil yields comparable to the literature. The calibration of biomass (Arundo) feed rate found to be 35 g/h per RPM of the biomass dosing auger, were the sand flow rate was 400 g/h per RPM of the HTM dosing auger at a constant reactor speed of 50 RPM. The flow rate of carrier gas i.e. the inert gas (high purity nitrogen) was maintained at approx. 0.24 LPM (standard liters per minute).

Table 4.1 Experimental matrix

Particle size (range)	**Temperature**	**Thermal Pretreatment**	**Mineral Pretreatment**
Microns	**ºC**	**Mass loss**	**Wet sifting**
850-1000	500	0 (Raw)	No
425-850	500	0 (Raw)	No
< 425	500	0 (Raw)	No
425-850	470	0 (Raw)	No
425-850	500	0 (Raw)	No
425-850	530	0 (Raw)	No
425-850	500	0 (Raw)	Yes
425-850	500	0 (Raw)	No
425-850	500	7%	Yes
425-850	500	7%	No
425-850	500	16.5%	Yes
425-850	500	16.5%	No
425-850	500	23%	Yes
425-850	500	23%	No
425-850	500	29.4%	Yes
425-850	500	29.4%	No
425-850	500	37.8%	Yes
425-850	500	37.8%	No

Table 4.2 Moisture and ash content of vs. size fractions. (Donepudi, Desai et al. 2017)

Size	Moisture (%)	Ash (%)
< 425 microns	3.8	15.2
425-850 microns	3.5	10.0
850-1000 microns	3.7	7.4

4.1.1 Influence of particle size

Three different feedstock particle sizes i.e. less than 425 microns, 425-850 microns and 850-1000 microns were used. To maintain consistency and less variables, the speed of the reactor was kept constant at 50 RPM for all the runs with a reaction temperature of 500 ºC. Table 4.3 shows the results from these particle size experiments. It can be seen that the size did not affect the bio-oil yield, however there is a change in char yields which had decreased with size. In other words, larger particles had produced more char indicating incomplete reaction due to less residence time in accordance with their size and/or poor mixing/contact with the HTM. It can be understood from these experiments that smaller feedstock particle sizes are to be selected to obtain good oil yields with less char. However there is a tradeoff between choosing right size and its effect on process influencing factors such as flow and mineral content. Through several experiments it was found that the for AD, the particle size in the between 425-850 microns have proven best in flowing capabilities (lower chances of forming flow inhibiting bridges inside the system's storage bins and gravity assisted drop tubes) and reduced mineral content compared to the next lowest size i.e. less than 425 microns (see Table 4.2). This is the reason 425-850 micron particles are chosen for the next study dealing with the effect of reaction temperatures.

Table 4.3 Condensable and bio-char yields (based on dry-ash-free basis) obtained for AD at different size fractions, pyrolyzed at 500ºC. (Donepudi, Desai et al. 2017)

Size	Char (%)	Condensable (%)
< 425 microns	20.3	51.6
425-850 microns	24.6	51.9
850-1000 microns	26.9	50.1

4.1.2 Effect of reaction temperature

The experiments to find the effect of reaction temperature were done by varying the pyrolysis zone temperature (470 ºC to 530 ºC) with reactor speed (at 50 RPM) and particle size (425-850 microns) being constant. Table 4.4 shows the results of char and bio-oil yield from these experiments. From the results it can be inferred that the reaction temperatures of 470 ºC and 500 ºC have produced similar bio-oil yields, whereas the yield decreased by 7% for reaction temperature of 530 ºC. From this study, the optimal reaction temperatures for Arundo were found to be in between 470-500 ºC, which are considered low temperatures for fast pyrolysis to obtain high bio-oil yields. The high mineral content of AD (Table 4.2) could be a factor helping the cause of better oil yields at lower temperatures by acting as catalysts, increasing the cracking reactions (Patwardhan, Satrio et al. 2010). The char yields were completely different and cannot be related to the bio-oil yield behavior with temperatures. The reaction temperatures of 470 ºC and 530 ºC had yielded almost the same amount of char, whereas its yield was increased when the reaction temperature was 500 ºC. The factors influencing this char behavior are unknown and is considered for future work.

Table 4.4 Condensable and bio-char yields (based on dry-ash-free basis) obtained for AD at temperatures 470-530ºC. (Donepudi, Desai et al. 2017)

Temperature	Char (%)	Condensable (%)
470 °C	22.1	50.6
500 °C	26.9	51.0
530 °C	21.1	46.3

4.2 Effect of minerals on fast pyrolysis yields

Minerals play a crucial role in fast pyrolysis. From previous chapter it was concluded that their presence can lead to a lot of catalytic reactions, which then encourage the formation of secondary reactions thereby reducing the amount of levoglucosan (useful fuel product of fast pyrolysis) and might affect the total yield. Also, the literature suggests that a two stage fast pyrolysis (torrefaction followed by fast pyrolysis) produces optimal yields compared to that of a single stage fast pyrolysis. To study the effect of minerals on fast pyrolysis Arundo Donax (AD) was chosen as it has very high inorganic content, primarily K (see the mineral distribution in Table 4.5). AD was thermally pretreated (torrefied) to obtain product with various mass losses i.e. 7%, 16.5%, 23% and 29.4% (compared to original mass). These thermally pretreated feedstocks were divided into two fractions to be designated as demineralized and non-demineralized. The aqueous demineralization technique using high shear mixer discussed in Chapter 3 was used to reduce the amount of minerals (soluble minerals) from the torrefied feedstocks (see Table 4.6 for demineralization parameters used for this study). Then these pretreated feedstocks (both demineralized and non-demineralized) were processed by fast pyrolysis using sand as HTM at a reaction temperature of 500 ºC. The results can be seen in Figures 4.1 and 4.2.

Table 4.5 Ash characterization of Arundo Donax (Donepudi, Desai et al. 2017)

Minerals	**Chemical formula**	**As received (%)**
Silica	SiO2	47.34
Alumina	Al2O3	2.91
Titania	TiO2	0.25
Lime	CaO	6.00
Ferric Oxide	Fe2O3	4.06
Potassium Oxide	**K2O**	**25.53**
Magnesium Oxide	MgO	2.29
Sodium Oxide	Na2O	1.78
Sulfur Trioxide	SO3	2.76
Phosphorus Pentoxide	P2O5	1.88
Barium Oxide	BaO	0.05
Manganese Dioxide	MnO2	0.09
Strontium Oxide	SrO	0.03
Undetermined		5.03

Table 4.6 Demineralization parameters

Biomass to water mass ratio	1:20
High shear mixer rotor speed	5000 RPM
Residence time	5 minutes
Drying temp. post demineralization	105 ºC

4.3 Effect of torrefaction severities on fast pyrolysis yields

From literature it has been concluded that torrefaction is one of the important pretreatment methods to be used for fast pyrolysis of biomass, where the inclusion of it is known as a multistage fast pyrolysis process to help optimize the yields. Several experiments had been done in this work which will elucidate the effect of torrefaction on fast pyrolysis yields.

Arundo Donax (AD) and Forest residues (FR) had been chosen for this work. The raw AD is dried, ground and size fractioned to obtain particle sizes in the range of 450 to 850 microns. Then the raw AD is torrefied using the fast pyrolysis system to obtain five different mass losses (wt% compared to original mass) i.e. 7%, 16.5%, 23%, 29.4% and 37.8%. Raw and torrefied FR samples was processed at Idaho National Laboratory and were shipped to Michigan Technological University for testing. The particle size of the FR samples was < 450 microns. The mass loss of the torrefied FR was 11% (wt%, compared to original mass). Part of all the torrefied samples were demineralized using the novel mineral removal technique with the high shear mixer using the parameters listed on Table 4.6. For reference, the list of properties of different samples used for this analysis is provided in Table 4.7. After torrefaction and demineralization, in the next stage of the process these individual 'torrefied' and 'torrefied-demineralized' samples (AD and FR) were processed with fast pyrolysis parameters listed on Table 3.6 to obtain bio-oil, char and non-condensable gases.

Table 4.7 Properties of different samples used for analysis

				After Demineralization	
Name	**Mass loss**	**Ash**	**Moisture**	**Ash**	**Moisture**
Arundo Donax					
R.AD~0%	0.0%	17.1%	6.8%	10.1%	2.4%
T.AD~7%	7.0%	12.4%	3.7%	6.1%	2.3%
T.AD~15%	16.5%	14.2%	3.7%	8.3%	3.2%
T.AD~25%	23.0%	15.9%	4.3%	9.5%	2.9%
T.AD~30%	29.4%	18.2%	3.6%	12.9%	3.8%
T.AD~40%	37.8%	20.9%	3.8%	13.1%	5.1%
Forest Residues					
R.FR~0%	0.0%	3.2%	2.6%	N/A	N/A
T.FR~15%	11.0%	2.5%	2.2%	2.3%	4.5%
R=Raw, T=Torrefied, AD=Arundo Donax, FR=Forest Residues					

Figures 4.1 and 4.2 show the results of bio-oil yields in terms of as is and dry ash free basis (d.a.f) respectively from processing different samples In both the cases the bio-oil yield tend to decrease with increment of mass loss, which is an obvious result of losing some liquid/condensable yield during torrefaction process. However, the yields from torrefied-demineralized samples is slightly higher compared to only torrefied samples. The increase in yield was hypothesized to be a resultant of decreased catalytic reactions from low mineral content and/or the reduced particle size from comminution during high shear processing which will increase the surface area (which increases the K/s) of the product thereby increasing the chance of complete thermal conversion of the sample into liquid yield.

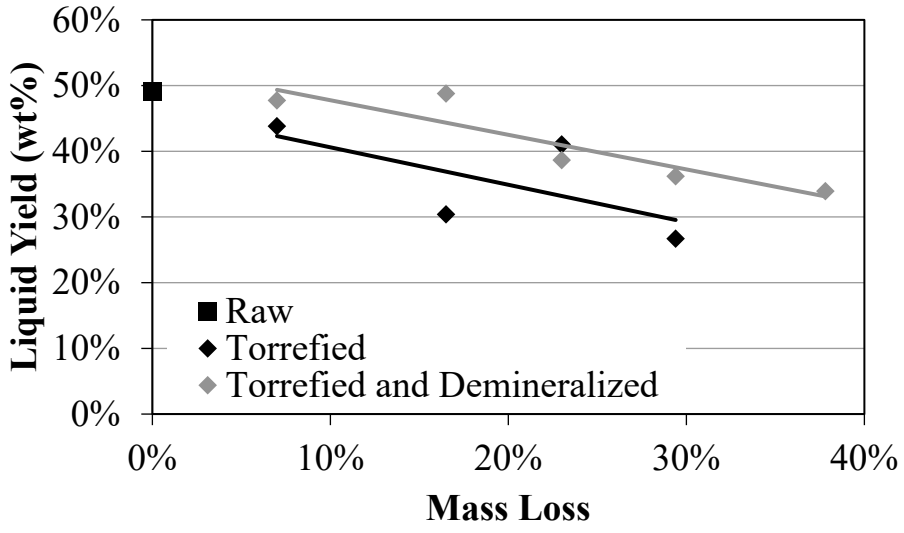

Figure 4.1 As-is liquid yields of AD samples compared to torrefaction mass loss

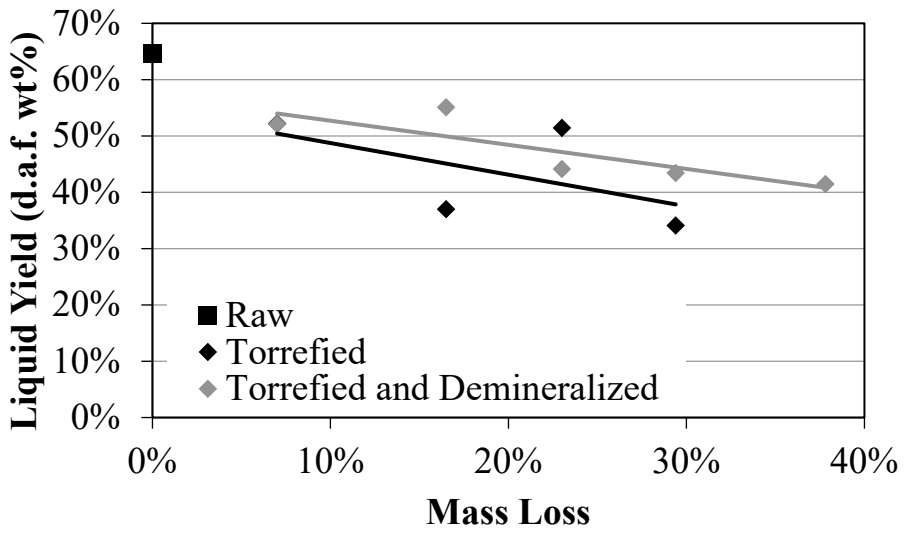

Figure 4.2 Liquid yields of AD samples based on dry ash free basis compared to torrefaction mass loss

It is interesting to notice that the yields did not change with torrefaction and demineralization compared to the raw samples when we compare the yield to the original mass as seen in Figure 4.3. However, the quality of oils might differ as torrefaction assists in removal of undesirable compounds like organic acids and which could be quantified by oil speciation by using gas chromatography.

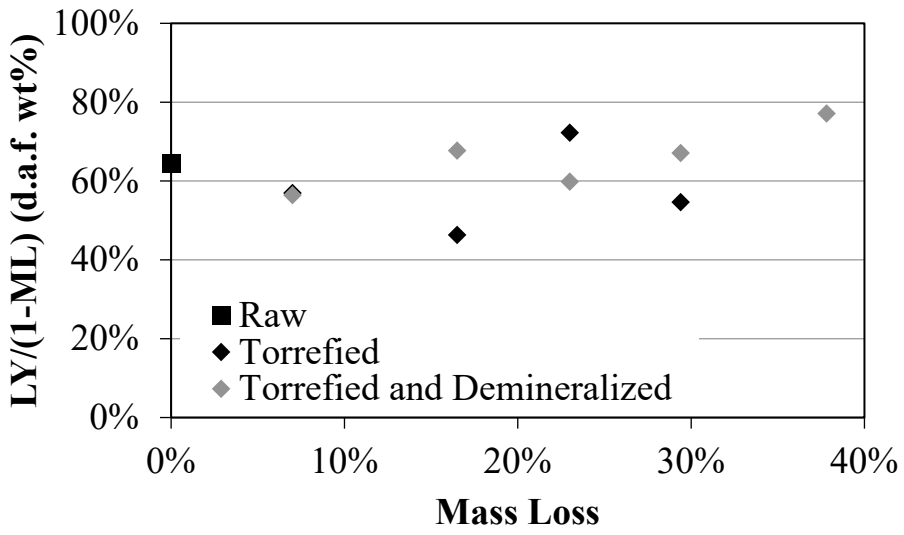

Figure 4.3 Liquid yield of AD samples (original mass basis) compared to torrefaction mass loss

Table 4.8 represents the results for comparatively low mineral content woody feedstock i.e. forest residue samples, where it can be observed that the results were similar to that of AD samples, however the torrefied-demineralized sample accounted for comparatively high bio-oil yield compared to raw and torrefied samples.

Table 4.8 Liquid yields of Forest residue samples

	Liquid yield (wt%)		
Sample	As-is	Dry ash free basis	Original mass basis
Raw	54.9%	58.27%	58.27%
Torrefied	45.1%	47.26%	53.42%
Torrefied-demineralized	53.5%	65.36%	65.01%

5 Conclusions and future work

The main objectives of this work were to develop and explore pretreatment methods for fast pyrolysis to enable the use of low cost feedstocks and to operate a novel cost effective reactor to achieve efficient conversion. All of these were completed by this extensive work and it yielded several important conclusions. This work demonstrates the applicability of pretreated biomass feedstock for production of enhanced pyrolysis oil.

From the literature survey it was inferred that the major hindrance of using low cost feedstocks for bio-oil production is its high mineral content. The high mineral content biomass obtained lower bio-oil yields compared to feedstocks with lower mineral content. The SEM study found that most of the minerals in biomass form colonies or clusters within the biomass fibers and the size of these agglomerated minerals are observed to be in range of 2 to 20 microns. This observation led to the use of dry sifting technique, where the biomass feedstock is size separated with a stack of sieves ranging from smallest to highest mesh sizes. It was concluded that the sifting reduces the mineral content of biomass, where the majority of the minerals are concentrated in lower size fractions. However, the efficiency of removal was observed mediocre. The next innovation of this work was to use shear forces to chop the minerals from the biomass fibers using a wet medium. This work has successfully demonstrated that the mineral content of any biomass feedstock can be reduced to a lower or acceptable levels by a simple high shear process followed by mild thermal pretreatment. The high shear mineral reduction technique used in this work is comparatively superior to traditional leaching techniques in terms of water and time requirements. Shear forces help in efficiently

dislodging the mineral colonies inside biomass fibers, thereby assisting in their effective removal. It was concluded that thermally pretreated biomass (even mild) yields better mineral removal efficiencies compared processing raw biomass and it increases with severity of the thermal pretreatment. The proposed high shear mineral reduction technique can be applied to both herbaceous and woody biomass feedstocks. The high shear process may help in comminution of biomass particles, effectively reducing further grinding energy. The proposed high shear process in aqueous medium can be effectively used to minimize/eliminate dust hazard during biomass comminution.

This work demonstrated that the novel paddle reactor is capable of high quality mixing, which can produce bio-oil yields comparable to the popular fluid bed reactors. This novel reactor was capable of achieving very high heating rates required for fast pyrolysis. It was also capable of sustaining its heating rates without the use of any heat transfer medium (HTM) and demonstrated that it can produce comparable bio-oil yields. The major drawback of using sand as an HTM was that it caused wear and tear of the reactor paddle auger, however the novel design is capable of handling other HTM material like shots. The current configuration suffers with feedstock flow-ability issues (primarily at feeding sections) and is an area for future R&D. Comminution of the biomass particles was observed when transferred through the reactor section with the paddle auger. The major advantage of this system is that it is cost effective and could easily be scaled up compared to traditional fluid bed systems.

The fast pyrolysis work yield several conclusions. It was observed that the particle size of biomass has no or minimal effect on bio-oil yields, however it is affected by the reaction

temperatures and was observed that a reaction temperature of 500 ºC was optimal for several biomass feedstocks. It was concluded that multistage pyrolysis with torrefaction yields better product compared to single stage pyrolysis. Torrefaction was considered one of the important pretreatments of biomass as it reduces the grinding energy, improves mineral reduction efficiencies and produce pretreated feedstock that would yield bio-oils less in acids which helps in reducing the corrosive nature and improving its stability. The bio-oil from torrefied biomass reduced with increase of torrefaction severities, however when compared to their original mass the bio-oil yields were more consistent and were comparable to yield from processing raw biomass. This work affirms the literature finding that fractional/multistage pyrolysis (for example a 2 stage process consists of, stage-1: torrefaction and stage-2: fast pyrolysis) is the best fast pyrolysis method to obtain stable bio-oils with optimal yields. Mineral content in biomass negatively effects the bio-oil yield and it was observed that reducing the mineral content of the feedstock increased the bio-oil yield.

Overall, this work provides a strong basis for the use of low cost feedstocks for bio-oil production from fast pyrolysis.

This work quantifies the impacts of several pretreatment methods on fast pyrolysis. However, there were several aspects of different methods or processes which still need further exploration for complete explanation of several hypotheses made during the work.

The following are some aspects for the future work.

- Investigation of different mineral rich low cost feedstocks and compare how the results vary with this work and thereby effectively quantifying the applicability of the proposed processes.
- Investigation on the scalability of the novel paddle reactor.
- Quantification of the quality of bio-oils produced by GC-MS analysis, where the samples are tested for acid, water and sugar levels at different stages of maturity of the stored oils.
- To explore new techniques to improve flow-ability of biomass feedstocks (primarily fibrous) in the novel reactor and effective throughput.
- Investigation of the applicability and effect of different HTM materials
- Investigating the end-user applicability of these bio-oils with or without fractionation (example: testing them in I.C engines)

6 References

Acharya, B., et al. (2012). "A review on advances of torrefaction technologies for biomass processing." Biomass Conversion and Biorefinery **2**(4): 349-369.

Adjaye, J. and N. Bakhshi (1995). "Production of hydrocarbons by catalytic upgrading of a fast pyrolysis bio-oil. Part II: Comparative catalyst performance and reaction pathways." Fuel Processing Technology **45**(3): 185-202.

Adjaye, J. D. and N. Bakhshi (1995). "Production of hydrocarbons by catalytic upgrading of a fast pyrolysis bio-oil. Part I: Conversion over various catalysts." Fuel Processing Technology **45**(3): 161-183.

Agblevor, F. and S. Besler-Guran (2002). "Fractional pyrolysis of biomass for high-valued products." Gas **40**: 4.

Arias, B., et al. (2008). "Influence of torrefaction on the grindability and reactivity of woody biomass." Fuel Processing Technology **89**(2): 169-175.

Asadieraghi, M. and W. M. A. W. Daud (2014). "Characterization of lignocellulosic biomass thermal degradation and physiochemical structure: Effects of demineralization by diverse acid solutions." Energy Conversion and Management **82**: 71-82.

Aslam, U., et al. (2016). "Effect of demineralization on the physiochemical structure and thermal degradation of acid treated indigenous rice husk." Polish Journal of Chemical Technology **18**(3): 117-121.

Aubin, H. and C. Roy (1990). "Study on the corrosiveness of wood pyrolysis oils." Petroleum Science and Technology **8**(1): 77-86.

Baxter, L. L., et al. (1998). "The behavior of inorganic material in biomass-fired power boilers: field and laboratory experiences." Fuel Processing Technology **54**(1): 47-78.

Bergman, P. C., et al. (2005). "Torrefaction for biomass co-firing in existing coal-fired power stations." Energy Centre of Netherlands, Report No. ECN-C-05-013.

Boucher, M., et al. (2000). "Bio-oils obtained by vacuum pyrolysis of softwood bark as a liquid fuel for gas turbines. Part II: Stability and ageing of bio-oil and its blends with methanol and a pyrolytic aqueous phase." Biomass and Bioenergy **19**(5): 351-361.

Brady, M., et al. (2017). "Corrosion of stainless steels in the riser during co-processing of bio-oils in a fluid catalytic cracking pilot plant." Fuel Processing Technology **159**: 187-199.

Branca, C., et al. (2014). "Effects of the torrefaction conditions on the fixed-bed pyrolysis of Norway spruce." Energy & Fuels **28**(9): 5882-5891.

Bridgeman, T., et al. (2010). "An investigation of the grindability of two torrefied energy crops." Fuel **89**(12): 3911-3918.

Bridgwater, A. V. (2012). "Review of fast pyrolysis of biomass and product upgrading." Biomass and Bioenergy **38**: 68-94.

Brown, J. N. and R. C. Brown (2012). "Process optimization of an auger pyrolyzer with heat carrier using response surface methodology." Bioresource Technology **103**(1): 405-414.

Brown, R. C. and J. Holmgren (2009). "Fast pyrolysis and bio-oil upgrading." Gas **13**: 25.

Brown, R. C., et al. (2001). Pretreatment processes to increase pyrolytic yield of levoglucosan from herbaceous feedstocks.

Cai, W., et al. (2017). "Effects of Torrefaction on the Physicochemical Characteristics of Sawdust and Rice Husk and Their Pyrolysis Behavior by Thermogravimetric Analysis and Pyrolysis–Gas Chromatography/Mass Spectrometry." Energy & Fuels **31**(2): 1544-1554.

Carpenter, D., et al. (2014). "Biomass feedstocks for renewable fuel production: a review of the impacts of feedstock and pretreatment on the yield and product distribution of fast pyrolysis bio-oils and vapors." Green Chemistry **16**(2): 384-406.

Chaala, A., et al. (2004). "Colloidal properties of bio-oils obtained by vacuum pyrolysis of softwood bark: aging and thermal stability." Energy & Fuels **18**(5): 1535-1542.

Chen, D., et al. (2016). "Combined pretreatment with torrefaction and washing using torrefaction liquid products to yield upgraded biomass and pyrolysis products." Bioresource Technology.

Chiaramonti, D., et al. (2003). "Development of emulsions from biomass pyrolysis liquid and diesel and their use in engines—Part 1: emulsion production." Biomass and Bioenergy **25**(1): 85-99.

Chiaramonti, D., et al. (2003). "Development of emulsions from biomass pyrolysis liquid and diesel and their use in engines—Part 2: tests in diesel engines." Biomass and Bioenergy **25**(1): 101-111.

Choi, J. H., et al. (2017). "Effects of water-washing Saccharina japonica on fast pyrolysis in a bubbling fluidized-bed reactor." Biomass and Bioenergy **98**: 112-123.

Colin, B., et al. (2017). "Quantification of the torrefaction effects on the grindability and the hygroscopicity of wood chips." Fuel **197**: 232-239.

Czernik, S. and A. Bridgwater (2004). "Overview of applications of biomass fast pyrolysis oil." Energy & Fuels **18**(2): 590-598.

Czernik, S., et al. (1994). "Stability of wood fast pyrolysis oil." Biomass and Bioenergy **7**(1): 187-192.

Dhyani, V. and T. Bhaskar (2017). "A comprehensive review on the pyrolysis of lignocellulosic biomass." Renewable Energy.

Di Blasi, C. (1996). "Kinetic and Heat Transfer Control in the Slow and Flash Pyrolysis of Solids." Industrial & Engineering Chemistry Research **35**(1): 37-46.

Diebold, J. P. (1999). A review of the chemical and physical mechanisms of the storage stability of fast pyrolysis bio-oils, National Renewable Energy Lab., Golden, CO (US).

Donepudi, Y., et al. (2017). Enhanced bio-oil from arundo donax. Michigan Technological University.

Donepudi, Y., et al. (2017). Biomass pretreatment methods for fast pyrolysis

Dupont, C., et al. (2014). "Heat capacity measurements of various biomass types and pyrolysis residues." Fuel **115**: 644-651.

Dutta, A., et al. (2015). Process Design and Economics for the Conversion of Lignocellulosic Biomass to Hydrocarbon Fuels. Thermochemical Research Pathways

with In Situ and Ex Situ Upgrading of Fast Pyrolysis Vapors, NREL (National Renewable Energy Laboratory (NREL), Golden, CO (United States)).

EIA (2016). International energy outlook 2016.

EIA (2017). Total Energy

Elliott, D. C. (1994). "Water, alkali and char in flash pyrolysis oils." Biomass and Bioenergy **7**(1): 179-185.

Eom, I.-Y., et al. (2012). "Study on the thermal decomposition features and kinetics of demineralized and inorganic metal-impregnated lignocellulosic biomass." Journal of Industrial and Engineering Chemistry **18**(6): 2069-2075.

Eom, I.-Y., et al. (2013). "Comparison of pyrolytic products produced from inorganic-rich and demineralized rice straw (Oryza sativa L.) by fluidized bed pyrolyzer for future biorefinery approach." Bioresource Technology **128**: 664-672.

Eom, I.-Y., et al. (2011). "Characterization of primary thermal degradation features of lignocellulosic biomass after removal of inorganic metals by diverse solvents." Bioresource Technology **102**(3): 3437-3444.

Fratini, E., et al. (2006). "SANS analysis of the microstructural evolution during the aging of pyrolysis oils from biomass." Langmuir **22**(1): 306-312.

Haynes, W. M. (2012). CRC handbook of chemistry and physics, CRC Press.

Henrich, E., et al. (2016). "Fast pyrolysis of lignocellulosics in a twin screw mixer reactor." Fuel Processing Technology **143**: 151-161.

Howe, D., et al. (2015). "Field-to-Fuel Performance Testing of Lignocellulosic Feedstocks: An Integrated Study of the Fast Pyrolysis–Hydrotreating Pathway." Energy & Fuels **29**(5): 3188-3197.

Hwang, H., et al. (2013). "Fast pyrolysis of potassium impregnated poplar wood and characterization of its influence on the formation as well as properties of pyrolytic products." Bioresource Technology **150**: 359-366.

Ingram, L., et al. (2007). "Pyrolysis of wood and bark in an auger reactor: physical properties and chemical analysis of the produced bio-oils." Energy & Fuels **22**(1): 614-625.

Jenkins, B., et al. (2003). "Biomass leachate treatment by reverse osmosis." Fuel Processing Technology **81**(3): 223-246.

Jiang, S., et al. (2017). "Effects of thermal pretreatment and ex-situ grinding on the pyrolysis of mallee wood cylinders." Fuel Processing Technology **159**: 211-221.

Jones, S., et al. (2013). Process design and economics for the conversion of lignocellulosic biomass to hydrocarbon fuels: fast pyrolysis and hydrotreating bio-oil pathway, National Renewable Energy Laboratory (NREL), Golden, CO.

Kenney, K. L., et al. (2013). "Understanding biomass feedstock variability." Biofuels **4**(1): 111-127.

Klemetsrud, B., et al. (2016). "Characterization of Products from Fast Micropyrolysis of Municipal Solid Waste Biomass." ACS Sustainable Chemistry & Engineering **4**(10): 5415-5423.

Klinger, J., et al. (2015). "Unified kinetic model for torrefaction–pyrolysis." Fuel Processing Technology **138**: 175-183.

Liu, Z., et al. (2017). "Influence of Alkali and Alkaline Earth Metallic Species on the Phenolic Species of Pyrolysis Oil." BioResources **12**(1): 1611-1623.

Mante, O. D., et al. (2012). "The influence of recycling non-condensable gases in the fractional catalytic pyrolysis of biomass." Bioresource Technology **111**(Supplement C): 482-490.

Meier, D., et al. (2003). Chemical stability of wood fast pyrolysis liquids, CPL Press: Newbury, UK**:** 221-228.

Messina, L. G., et al. (2016). "Effect of mineral matter removal on pyrolysis of wood sawdust from an invasive species." Energy Sources, Part A: Recovery, Utilization, and Environmental Effects **38**(4): 542-548.

Mohan, D., et al. (2006). "Pyrolysis of wood/biomass for bio-oil: a critical review." Energy & Fuels **20**(3): 848-889.

NIST Quartz (SiO2). USA, National Institute of Standards and Technology.

Nokkosmäki, M., et al. (2000). "Catalytic conversion of biomass pyrolysis vapours with zinc oxide." Journal of Analytical and Applied Pyrolysis **55**(1): 119-131.

Oasmaa, A. and S. Czernik (1999). "Fuel oil quality of biomass pyrolysis oils state of the art for the end users." Energy & Fuels **13**(4): 914-921.

Oasmaa, A. and E. Kuoppala (2003). "Fast Pyrolysis of Forestry Residue. 3. Storage Stability of Liquid Fuel." Energy & Fuels **17**(4): 1075-1084.

Oasmaa, A., et al. (1997). "Physical characterisation of biomassbased pyrolysis liquids Application of standard fuel oil analyses. 1997." VTT OFFSETPAINO.

Oudenhoven, S., et al. (2013). "Demineralization of wood using wood-derived acid: Towards a selective pyrolysis process for fuel and chemicals production." Journal of Analytical and Applied Pyrolysis **103**: 112-118.

Patwardhan, P. R., et al. (2010). "Influence of inorganic salts on the primary pyrolysis products of cellulose." Bioresource Technology **101**(12): 4646-4655.

Pfitzer, C., et al. (2016). "Fast Pyrolysis of Wheat Straw in the Bioliq Pilot Plant." Energy & Fuels **30**(10): 8047-8054.

Phanphanich, M. and S. Mani (2011). "Impact of torrefaction on the grindability and fuel characteristics of forest biomass." Bioresource Technology **102**(2): 1246-1253.

Puy, N., et al. (2011). "Valorisation of forestry waste by pyrolysis in an auger reactor." Waste management **31**(6): 1339-1349.

Rabier, F., et al. (2006). "Particle density determination of pellets and briquettes." Biomass and Bioenergy **30**(11): 954-963.

Saddawi, A., et al. (2012). "Commodity fuels from biomass through pretreatment and torrefaction: effects of mineral content on torrefied fuel characteristics and quality." Energy & Fuels **26**(11): 6466-6474.

Salehi, E., et al. (2011). "Bio-oil from sawdust: effect of operating parameters on the yield and quality of pyrolysis products." Energy & Fuels **25**(9): 4145-4154.

Sirijanusorn, S., et al. (2013). "Pyrolysis of cassava rhizome in a counter-rotating twin screw reactor unit." Bioresource Technology **139**: 343-348.

Skone, T. J. (2012). Role of alternative energy sources: pulverized coal and biomass co-firing technology assessment, National Energy Technology Laboratory.

Thompson, V. S., et al. (2017). "Optimizing Biomass Feedstock Blends with Respect to Cost, Supply, and Quality for Catalyzed and Uncatalyzed Fast Pyrolysis Applications." BioEnergy Research: 1-13.

Tonn, B., et al. (2011). "Influence of leaching on the chemical composition of grassland biomass for combustion." Grass and Forage Science **66**(4): 464-473.

Trendewicz, A., et al. (2015). "Evaluating the effect of potassium on cellulose pyrolysis reaction kinetics." Biomass and Bioenergy **74**: 15-25.

USDA (2017). Rural Employment and Unemployment.

Westerhof, R. J., et al. (2012). "Stepwise fast pyrolysis of pine wood." Energy & Fuels **26**(12): 7263-7273.

Westover, T. L., et al. (2013). "Impact of thermal pretreatment on the fast pyrolysis conversion of southern pine." Biofuels **4**(1): 45-61.

Wigley, T., et al. (2016). "A detailed product analysis of bio-oil from fast pyrolysis of demineralised and torrefied biomass." Journal of Analytical and Applied Pyrolysis.

Wigley, T., et al. (2016). "Pretreating biomass via demineralisation and torrefaction to improve the quality of crude pyrolysis oil." Energy **109**: 481-494.

Zhang, Q., et al. (2007). "Review of biomass pyrolysis oil properties and upgrading research." Energy Conversion and Management **48**(1): 87-92.

Zhang, S., et al. (2016). "Effects of water washing and torrefaction on the pyrolysis behavior and kinetics of rice husk through TGA and Py-GC/MS." Bioresource Technology **199**: 352-361.

Zhang, S., et al. (2005). "Upgrading of liquid fuel from the pyrolysis of biomass." Bioresource Technology **96**(5): 545-550.

Zheng, Y., et al. (2017). "Effect of the Torrefaction Temperature on the Structural Properties and Pyrolysis Behavior of Biomass." BioResources **12**(2): 3425-3447.

Zhou, S., et al. (2014). "Py-GC/MS Studies to Evaluate the Effect of Torrefaction Temperature on Pyrolysis Products of Douglas Fir and Hybrid Poplar Wood." Transactions of the ASABE **57**(6): 1751-1759.

Zinchik, S., et al. (2017). Evaluation of fast pyrolysis feedstock conversion with a mixing paddle reactor. Michigan Technological University and Idaho National Laboratory.

Zinchik, S., et al. (2017). Heat transfer analysis in a paddle reactor for biomass fast pyrolysis Michigan Technological University and Idaho National Laboratory.

A Copyright information

The figures 1.1, 1.2 and 1.3 are reprinted with permission from U.S. Energy Information Administration and U.S. Department of Agriculture. All the three figures are from U.S. federal publications and are considered public domain. The author acknowledges the work done by various government agencies and does not assume ownership of any material pertaining to these three figures.